ECO-Resort fully powered by Renewables in the Azores

HotelEco

Tom Franklin, Tomi Akinrinmade, Rahul Singh, Oscar Boardman

11/12/2023

Executive Summary

This proposal presents a comprehensive vision for a sustainable luxury resort in Sao Miguel, emphasising the integration of luxury with environmental sustainability. The resort, designed to blend in with the natural landscape, includes 17 villas, 2 dining venues, a main pool area, a spa, and direct beach access, all constructed using locally sourced, sustainable materials.

The main aspect of the project is its reliance on renewable energy, primarily solar power, supplemented by wind energy and geothermal energy sourced from the local grid. The resort's energy strategy is informed by a detailed technical analysis of solar farm simulations, wind turbine assessments, and the incorporation of geothermal energy, ensuring a reliable and sustainable energy supply. A singular 30m diameter wind turbine was sufficient for the back-up energy source. A key aspect of the project is the careful modelling of energy demand. This analysis is based on detailed tourism data and energy consumption patterns, allowing for efficient and effective planning of the resort's energy needs. This approach ensures that the energy systems are not only sustainable but also tailored to the specific requirements of the resort.

Another innovative aspect of the project is the use of battery storage systems, with a particular focus on repurposing electric vehicle (EV) batteries. This strategy is crucial for ensuring the reliability and consistency of the energy supply, particularly in a location subject to fluctuations in renewable energy generation. The batteries can store enough energy for 3 days’ worth of electricity supply.

The financial implications of implementing such advanced renewable energy systems are analysed in the report. This includes a comprehensive cost analysis and maintenance plan for the solar panels, batteries, and wind turbines, providing a clear understanding of the long-term financial sustainability of the project. The total cost of the wind turbines, solar, geothermal and batteries comes to €3M.

The report also investigates the creation of a microgrid system that integrates the various renewable energy sources. This section discusses the technical and operational challenges involved in managing such a system, including control mechanisms and issues related to compatibility and efficiency. The environmental and socio-economic impacts of the project are thoroughly assessed. This includes an evaluation of the resort's carbon footprint and its potential contribution to reducing greenhouse gas emissions. Additionally, the report highlights the socio-economic benefits, such as job creation and the promotion of sustainable tourism practices, which align with the broader goals of environmental conservation and community development.

Essentially, this proposal emphasises the resort's potential to serve as a model for combining luxury hospitality with environmental responsibility. It highlights the project's alignment with eco-friendly objectives and its role in advancing sustainable practices in the tourism industry. The report also opens discussions on the possibility of future expansions and technological integrations, indicating the project's forward-thinking approach and its potential as a blueprint for future sustainable developments in the hospitality sector.

1 Introduction

1.1 Scope

In the heart of the Azores archipelago, where untouched natural beauty meets unmatched luxury, this document proudly presents a visionary proposal - a luxury resort fully powered by renewable energy. This establishment embodies a harmonious fusion of sustainable living and relaxing comfort. Nestled on the pristine coastline of Sao Miguel, Praia da Viola, where the site previously was used for water mills. This proposal aims to present an eco-conscious haven where discerning travellers can immerse themselves in the island's splendour while leaving only the lightest of footprints. This luxury resort will have 17 villas with 2 restaurants, 2 bars, main pool area and a spa. The guests will also have access to the beach nestled below the site as shown in Figure. 1.

Figure 1: The topology of the resort site.

The aim of the resort is to create a stunning luxury resort that blends into the landscape to not ruin the natural beauty of the Sao Miguel coastline. Therefore, the building materials will be local and sustainable, with certified wood, recycled and rapidly renewable materials mainly being used for construction. Any trees cut down for the site were used in construction, a new tree was planted helping mitigate the environmental impact of tree removal. The layout of the resort is shown in Fig. 2(a), as illustrated, there are three different types of villa to choose from, with each one having its own garden.

Firstly, there are the standard coastal villas which have a beautiful view of the Atlantic Ocean. Then there are the family villas these are 2 stories high and were initially placed just behind the coastal villas as shown in Appendix A, however looking further into the topology of the sit in fig. 1 it is evident that a gorge is present thus they have been moved further back as shown in Fig. 2(a). On the 2nd floor of these family villas there is a stunning balcony that looks out onto the ocean, these villas also include a small pool for the kids. Then lastly the retreat villas, these are more exclusive and private where guests can enjoy their own jacuzzi. There are two of these along the coastline and three up in the hills which are even more private and raised so that guests have a balcony with a jacuzzi. The colour key along with Fig. 2(a) provides a more vivid representation picture of the resort’s appearance.

We are proposing three renewable energy sources for the resort; solar energy will be the main one. As shown in Fig. 2, a potential site for the solar panels is highlighted in green. Along with solar energy, both wind energy produced on site and geothermal imported from the grid will be power the resort. Section 2 describes the design of these three sources, Section 3 will provide detail on how these energy sources will work together, thereafter, Section 4 presents an impact analysis. One of our aims is to maximise sustainability, and with the location being a fair distance from civilisation self-sufficiency is key. Therefore, underneath the solar panels is an organic garden that will produce fruit and vegetables for the resort in tandem there will be an on-site reverse osmosis plant which will provide water that can be bottled in reusable glass bottles, both of these implementations will help reduce plastic waste and need for imports to the resort.

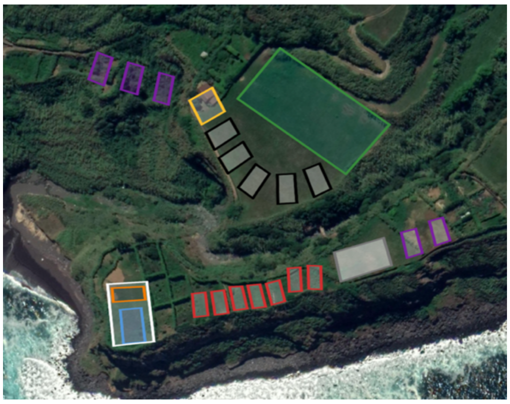

Fig 2(a): Layout of ECO-resort using Google Earth.

Colour	Structure	Dimensions
Red	Standard Coastal Villlas	30 X 55 ft
Black	Family Villas	40 X 65 ft
Purple	Retreat Villas	35 X 60 ft
White	Pool Area	145 X 95 ft
Blue	Infinity Pool	54 X 82 ft
Orange	Pool Bar & Restaurant	78 X 30 ft
Grey	Main Restaurant & Bar	120 X 70 ft
Yellow	Spa	60 X 60 ft
Green	Solar Panels & Organic garden	300 X 140 ft

Fig 2(b): Colour key with dimensions of villas/buildings.

1.2 Modelling of the resort's energy demand

Our approach initiated with a thorough analysis of energy consumption in similar resorts and hotels. By considering factors such as seasonal variations, we meticulously calculated an estimate for daily energy usage. To model the energy demand of the resort, a general guide was employed which is based on the hotel area (World Tourism Organization, 2011). It states that most hotels consume 200-400kWh/m^2/year. Based on the size of the buildings in Fig. 2(b), the area of the resort has been estimated to be 5650m^2. As the resort is sustainable and for simplicity, a lower bound was taken from the energy consumption range – 265kWh/ m^2/year, and therefore the resort's energy consumption was found to be 1500MWh per year. Using tourism data (Pimentel et al., 2020) we found that most hotels in the Azores run at an 80% capacity during the months of November through to March.

Taking these factors into consideration, a potential monthly energy consumption was derived and is illustrated below in Fig. 3(a). To model the daily energy consumption, the monthly energy consumption from Fig. 3(a) was divided by its respective number of days. Then, using statistics of the energy demand curve for a UK household (Pimm et al., 2018) we were able to model an approximation for the daily energy demand for the resort throughout the day. This was slightly altered during the daytime as we assume resort guests will be spending the majority of their time at the resort and not travelling too much, while the UK energy demand assumes most people to be away from the house during the daytime. Fig. 3(b) shows the potential energy demand throughout an average day.

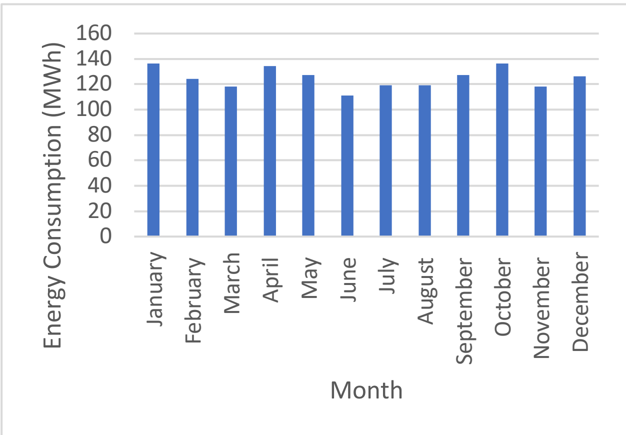

Fig 3(a): Potential monthly energy consumption of the resort

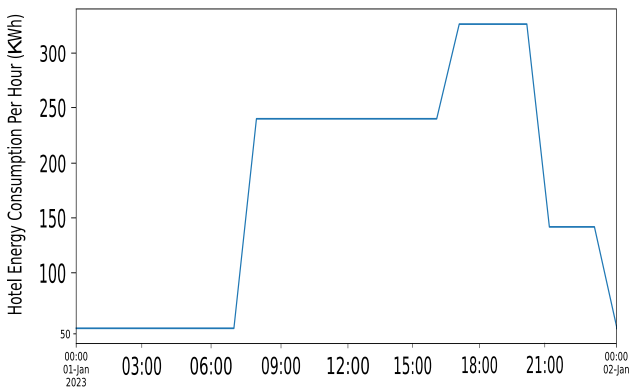

Fig. 3(b): Potential daily energy consumption of the resort.

2 Technical Analysis

In this section the three chosen renewable sources (solar, wind and geothermal) are further examined and discussed to show how they can potentially power the ECO-resort. Each renewable energy source is assessed based on the effectiveness of diverse design and modelling methods demonstrated for energy output. Through an in-depth evaluation of these renewable sources, the proposal aims to present the most effective and environmentally responsible energy solution for the ECO-resort.

2.1 Solar Energy

2.1.1 Introduction

Our solar farm, located at back of the resort with minimal obstructions, features a total of 1920 'Canadian Solar Hiku 410W' (CSI Solar Co., Ltd, 2023) modules in 8 arrays. We have decided to use efficient and budget friendly Solplanet 100kW inverters (Renewableshop.co.uk, 2023). The solar farm will produce 1045MWh annually and have a capacity of 787.2kW. Financially, we balance total expenditures at €357,169 for capital and €12,367 for operations and maintenance. We utilised the open-source software pvlib (Holmgren et al., 2018) for simulating photovoltaic system performance. The simulations were conducted using meteorological data obtained from PVGIS (EU Science Hub, n.d.).

The selection of the photovoltaic module and inverter parameters was performed with the goal of maximising energy output in the given environmental conditions.

2.1.2 Meteorological Data Collection

The hourly meteorological data, essential for simulating solar farm performance, was obtained using the PVGIS TMY generator (EU Science Hub., n.d.). This dataset encompasses key parameters such as Direct Normal Irradiance (DNI) in W/m², Diffuse Irradiance (DIF) in W/m², Global Horizontal Irradiance (GHI) in W/m², windspeed, and air temperature. The data spans the entirety of 2020 and was organised into an Excel spreadsheet for easy reference. The irradiance values represent the solar power incident on a unit area (per square meter). The significance of this irradiance data lies in its pivotal role in calculating various parameters crucial for the solar farm simulation.

2.1.3 Simulation of the Solar Farm

After obtaining the hourly meteorological data for the location, the solar zenith and azimuth were calculated hourly using an algorithm outlined by (Reda, I. and Andreas, A. 2004). The solar zenith and azimuth angles are used to describe the position of the sun in the sky relative to the solar array. This algorithm required the time of day, the location and altitude. Using the solar zenith and azimuth, the angle of incidence (AOI) of the solar vector on the solar module's surface was calculated. The equation developed by Sanida National Lablatories (PV Performance Modeling Collaborative (PVPMC), n.d.) represents this calculation for the AOI, this can be seen in equation 1.

$$AOI = \sec[(\cos(\theta_z)\cos(\theta_t) + \sin(\theta_z)\sin(\sin(\theta_t))\cos(\theta_A - \theta_{A,array})] \quad (1)$$

where θ_z and θ_A represent the solar zenith and azimuth angles, and θ_t and $\theta_{A,array}$ represent the tilt and azimuth angles of the array, all with units of degrees. Using Global Solar Atlas (Solargis, 2020), the optimum tilt of the array, θ_t and array azimuth angle, $\theta_{A,array}$ were found to be 28 and 180 degrees. The Incident Angle Modifier (IAM) was then calculated, this accounts for changes in solar cell performance based on the angle at which sunlight strikes the module surface. This was calculated using equation 2 below.

$$IAM = 1 - b(\sec(AOI) - 1) \quad (2)$$

where b represents a parameter to adjust the incidence angle modifier as a function of angle of incidence. The default value is 0.05, for more information on this refer to (Souka, A.F. and Safwat, H.H., 1966). Leveraging the IAM, the effective irradiance was calculated. This involves multiplying the Direct Normal Irradiance (DNI) (W/m^2) by the IAM and adding the Diffuse Irradiance (DIF) (W/m^2) which are taken from the meteorological data as show below in equation 3,

$$I_{eff} = (DNI \times IAM) + DIF \quad (3)$$

This comprehensive calculation represents the total irradiance I_{eff} reaching the solar modules in (W/m^2), considering both scattered sunlight and direct sunlight. Subsequently, the temperature of the module T_{module} was calculated throughout the year using the Faiman model (Faiman, D., 2008), with equation 4.

$$T_{module} = T_a + \frac{GHI}{U_0 + U_1 v}, \quad (4)$$

the Faiman model relies on key meteorological data, namely Global Horizontal Irradiance (GHI) in W/m², air temperature T_a in degrees Celsius, and wind speed (v) in m/s. Within this model, assumptions are made to determine the heat loss factor coefficients. The heat loss factor U_0, representing thermal losses without wind, is assumed to be 25 W/(Cm²), aligning with Faiman's considerations for silicon modules. Additionally, the wind-influenced heat loss factor U_1 is assumed to be 6.84 Ws/(Cm³), based on Faiman's assumptions. These coefficients play a crucial role in accurately finding the hourly module temperatures. Once the total irradiance reaching the solar modules and the module temperature variations are established, the calculation of DC and AC power outputs becomes feasible. To determine the DC power output of the modules, NREL's PVWatts DC power model is employed (Dobos, A, 2014)., as shown in Equation 5.

$$P_{dc} = \frac{I_{eff}}{1000} P_{dc0}[1 + \gamma_{pdc}(T_{module} - T_{ref})] \quad (5)$$

This model, integrates several key parameters including effective irradiance I_{eff}, module temperature T_{module}, nominal power of the modules at 1000 W/m² P_{dc0}, this measured in Watts, the temperature coefficient of power of the module γ_{pdc} $(\frac{1}{C})$, and the reference temperature (assumed to be 25°C), T_{ref}. After calculating the DC power output, P_{dc} (W) for a single module, the next step involved determining the AC power output from the inverter. The efficiency of the inverter α, is considered in this calculation, The inverter will convert DC to AC. This can be calculated as $P_{ac} = \alpha P_{dc}$, this is needed for the microgrids. To scale the module to the farm size. The farm area is 3901 m^2 and is based off the area shown in Fig. 2(a). This area was divided by the module area to get the total number of modules required to cover the entire farm. Once the total number of modules are calculated, the power output at hourly intervals can be calculated using equation 6. As the power is calculated at hourly timestamps in Watts, the energy produced is in Wh. The Python code used to simulate this solar farm can be seen in Appendix B.

$$Total\ Energy\ Output\ (Wh) = no\ of\ modules \times P_{ac} \tag{6}$$

2.1.4 Solar Module Selection

After understanding how to simulate the energy output of the farm, the subsequent step involved selecting the optimal solar module. To make an informed decision, a thorough comparison was conducted using the solar panel comparison table available on the ITS Technologies website (I.T.S Technologies, 2023b). The selection criteria prioritised modules with the lowest cost per watt, aligning with the overarching goal of maintaining cost-effectiveness for the solar farm, which serves as the primary energy source for the resort. This approach aims to enhance project feasibility and operational efficiency. To ensure accuracy in the comparison, all simulated solar farms shared an identical overall area.

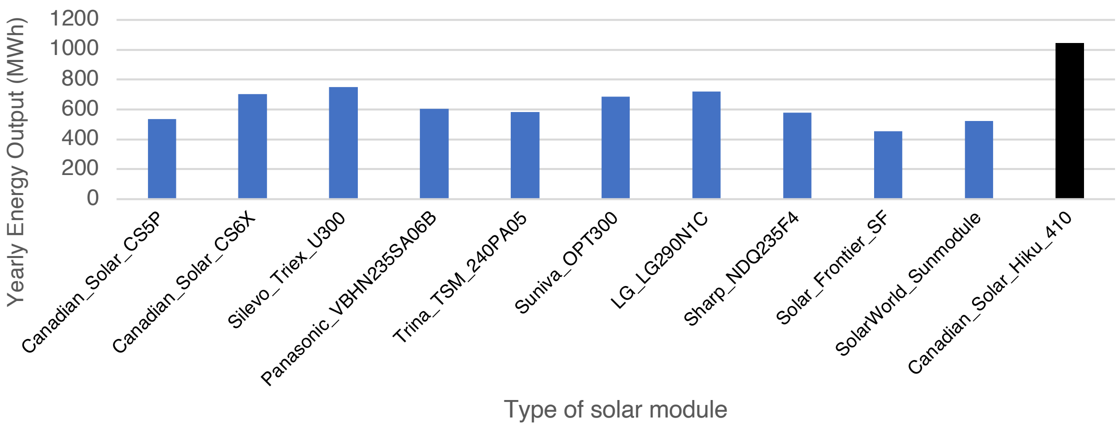

Fig. 4: Comparison of different solar modules.

Fig. 4 visually presents the outcome of the simulations, clearly indicating that the HiKU solar module significantly outperformed the alternative modules which were a mix of commercial mono-crystalline and poly-crystalline solar modules, in terms of energy output over the course of the year which was calculated using equation 6, and summing the hourly data over the year. Data in Appendix C shows the parameters of this Solar Module (CSI Solar Co., Ltd., 2023).

2.1.5 Solar Inverter Selection and Solar Farm Arrangement

After selecting the solar module and determining its area using the datasheet (Appendix C), it was then scaled to match the total farm area, the calculation shows that 1936 fit the farm area. However, to ensure safety and facilitate maintenance, the decision was made to have a slightly lower number, resulting in a final selection of 1920 solar modules. The total power output of the system was then computed by multiplying the number of modules by the rated power output P_{dc0} of 410W, yielding 787.2 kW for the total system power output. Given the commercial challenge of finding a solar inverter capable of handling this large amount of DC power, our suggested solution is to distribute the power input among 8 inverters, each with a rated power input of 100 kW. This arrangement translates to 240 solar modules per inverter (1920/8 = 240). The selected inverter, the Solplanet 100 kW, 3-phase, 10MPPT Inverter (Renewableshop.co.uk, 2023), has a maximum voltage input of 1100V and a maximum rated current input of 320A.

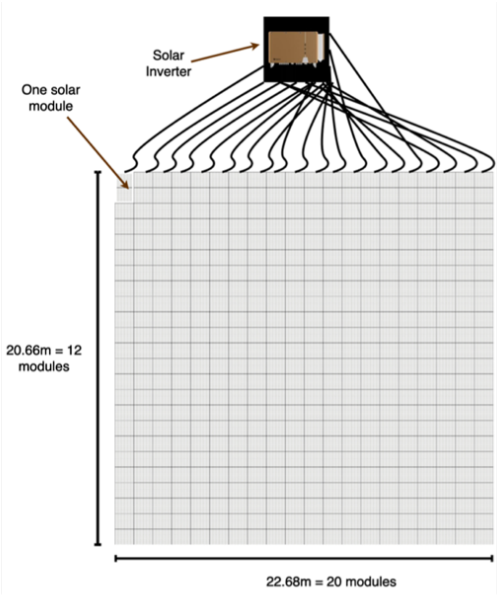

Figure 5: Solar array arrangement.

With these specifications in mind, the optimal series and parallel arrangement of the solar modules was determined based on the inverter's capacity to handle a large voltage input and a comparatively smaller current input. The chosen configuration resulted in 20 strings per inverter and 12 modules per string as shown in Figure 5. This arrangement yields a maximum current output from the of 157.8A ($12 \times 13.15 = 157.8A$), 13.15A being the operating current of the module, and a maximum voltage input of 630V ($31.2 \times 20 = 630V$), 31.2V is the operating voltage of the module these values can be found in Appendix B.

Figure 5 illustrates 1 solar array arrangement with the lines between the inverter and panels being the strings, there will be 8 of these to make up the full farm. The total area occupied by a single arrangement is 468.5 m², with the individual inverter's area measuring 0.63 m². Consequently, the entire solar farm will cover approximately 3753 m², leaving a buffer space of 148 m² within the allotted solar area.

2.1.6 Energy Outputs

Now that the most effective solar module and inverter have been selected for the solar farm. The total energy output can be calculated. The total energy output from the solar farm for the year is 1045MWh, this number was calculated by summing up the energy outputs hourly for the whole year from equation 6. The monthly energy output of the solar farm is shown below in Fig 6a. A simulation of 4 days in July was done and Fig. 6b below represents the energy produced hourly during each day. As seen, there is major energy production between the time periods of 8am and 6pm but almost nothing at any other time. Due to this uncertain energy production, we have decided to store any excess energy produced in batteries. Some days may produce much less than others also seen in Fig. 6b, July 1st produced much less than July 4th. Some energy needs to be stored for longer. The solar energy produced varies based on time of the year. Solar energy accounts for around 70% ($1045/1500 = 70\%$) of total energy production to supply the resort.

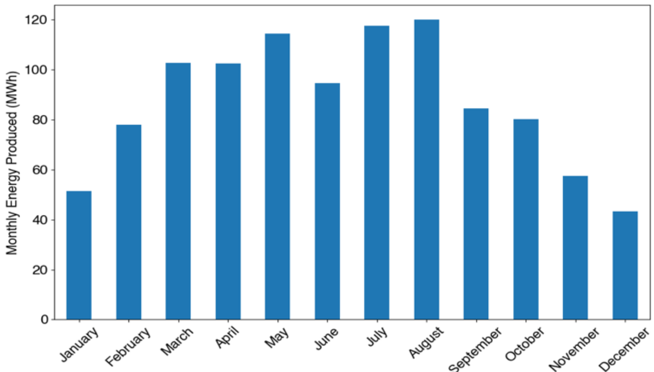

Fig. 6(a): Monthly solar energy output

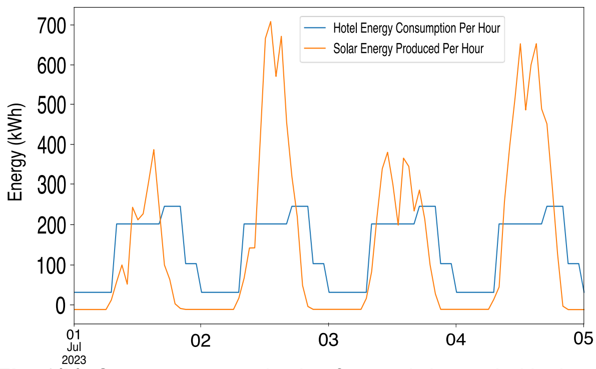

Fig: 6(b): Solar energy production from a 4-day period in July.

2.1.7 Cost and Maintenance analysis

Table 1 summarises the costs associated with the solar farm. The lifecycle of a solar panel is 25 years and for the inverter it is 5 years. Therefore, at these periods they will need to be replaced. The operation and maintenance cost is yearly and this encapsulates: Regular inspections, cleaning the solar panels, inspection of inverters to ensure safety, electrical system maintenance, security and safety of the solar panels and training for operation and maintenance staff.

Table 1: Price breakdown of the solar farm.

Cost of solar panel x 1920 (I.T.S Technologies. 2023a).	€163,922
Cost of inverter x 8 (Renewableshop.co.uk, 2023)	€8,342
Labour Cost (Sadler, R., 2023)	€184,904
Operation and Maintenance (Wiser et al., 2020))	€12,367
Total Cost	€369,536

2.2 Wind Energy

In this section, analysis was completed on different types of wind turbine and potential sites where the wind farm could be constructed. We are proposing a single 30m diameter 3-blade turbine that sits on the ridge above the ECO-resort site. The initial cost of €754K was roughly calculated and was one of the main reasons why wind wasn't chosen as the main source of renewable energy. Hence why smaller turbines were chosen for analysis and the 30m diameter made the most sense due to it producing an annual energy output of 462MWh, providing the necessary energy during months where solar didn't meet the resort's needs. The process of selection and modelling that was completed is explained in more detail below.

2.2.1 Wind patterns in Sao Miguel

As mentioned earlier, wind energy will play a pivotal role in sustainably powering the resort. With solar being the main source for energy, wind was mainly chosen as a backup. Extensive research was initially conducted on how different eco-resorts have fared when trying to optimise their renewable energy sources and reduce their carbon footprint. Evidence suggested that many struggled during periods when sunlight was scarce, such as winter months or night-time. This was mainly due to lack of exploration in other energy systems, like wind (Tierraatacama, 2023), (Six Senses, 2022). This was a focus for us as important findings were made during an evaluation of the weather conditions in the Azores (MeteoBlue, 2023). In the Azores, through the months of May to August most of the electricity will be supplied from the solar panels, refer to section 2.1.6. However, during the other months solar panels will be less effective, but looking at the figures below the wind tends to pick up during these months. Hence, why the combination of both wind and solar is effective due to how their inverse relationship with each other.

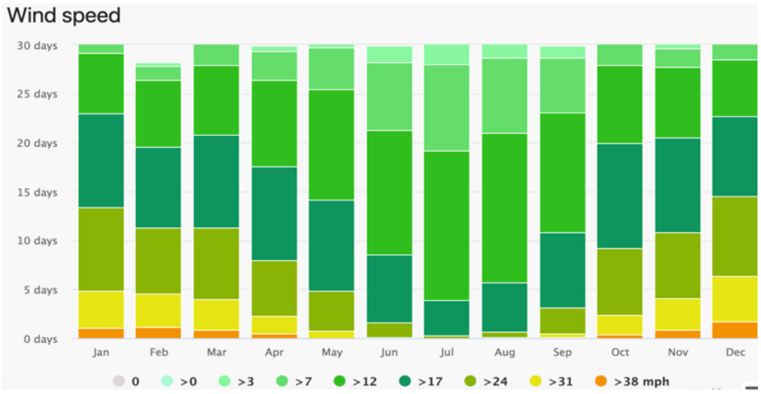

Fig.7(a): A variation of wind speed in the Azores.

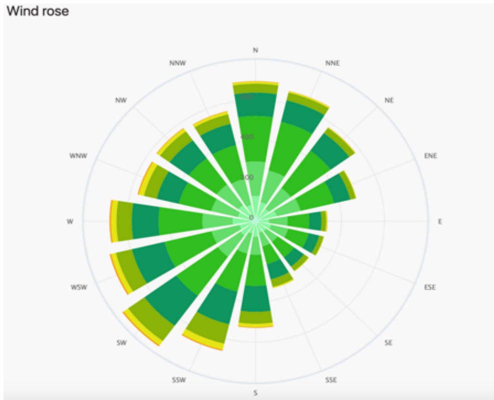

Fig. 7(b): A variation of wind direction in the Azores.

From October up until April there are very strong winds, and a yearly average of 22.93 mph means there is definitely enough to propose a wind farm. Looking at the directions of wind in the Azores region there is not a necessarily strong prevailing wind, therefore it might be more efficient for VAWTs to be used as they don't depend on direction. The possible types of wind turbine that could be used are compared in section 2.2.4.

Bearing in mind that this proposed wind farm would be to power an Eco-resort that prides itself on its beautiful landscape and views, a large wind farm may not be very aesthetic. Therefore, there are 2 different sites that could be of use these are compared in section 2.2.3.

2.2.2 Potential Wind-Farm Sites

Off-Shore:

The option of an off-shore wind farm could be the solution as most likely the guests won't be able to see the farm, thus not ruining the resorts beautiful aesthetics. The off-shore wind speed is usually greater than on-shore thus more power could be produced by the farm. There is also the consideration that marine life is severely impacted due to noise and vibrations. The price to build an off-shore wind farm may also be too expensive especially considering that it is not the main supplier to the resort.

On-Shore:
The possibility of an on-shore wind farm is limited without destroying the landscape. If the farm were to be placed in the same area given for the solar panels, there is a high chance the wind would be partially blocked by the surrounding hills thus reducing the potential power output. Another option would be to place the turbines on the ridge of the hill behind the resort, thus placing them in ideal spots to reduce any wind getting blocked. However, the required amount of turbines to produce the power needed may not fit on the ridge. One definite positive of an on-shore wind farm is that it would be considerably cheaper to construct.

2.2.3 Types of Wind Turbines

Firstly, the equation for wind power (Penn State, 2023) needs to be explained and the relative efficiency limits and laws that follow when calculating the power produced from a wind turbine. There is a limit to how much energy turbines can extract from wind. This is because, to maintain air flow over the aerofoils, some kinetic energy must be allowed to pass through the system. This is shown in equation 7,

$$P = \frac{1}{2} C_p \rho v_0^3 A \tag{7}$$

where P is power in W; C_p is the power coefficient and gives the fraction of available wind power the turbine is able to capture; ρ is the air density $(1.225\ \mathrm{kg/m^3})$; v_0^3 is the windspeed and A is the area swept by the turbine, for HAWTs and VAWTs these will be calculated slightly differently. The maximum theoretical efficiency limit of a turbine is 59.3%, also known as Betz's law. Below three different wind turbine design structures are compared, each one has been given height and diameter values that are interchangeable when implementing into our resort, however, for comparison purposes they have been given very different values to produce a range of different results.

Two-Blade Wind Turbine:
This two-bladed horizontal-axis wind turbine (HAWT) of height 40m and blade diameter 24m is a small turbine design. A reduced number of blades to the conventional 3-blade means the weight of the turbine is significantly reduced by roughly 30%, therefore making it easier to transport and construct. The smaller design would also reduce the social impact as the farm would be less of an eye sore for locals. So from equation 7, a power output of roughly 0.29 MW can be found for one turbine when using the average windspeed throughout the year and a C_p of 49%. A rough price of £208K is also found. An important note to make is that due to the 2-blade operating at highspeed the noise level is high so maybe not suitable for the on-site farm to avoid making it unpleasant for guests of the resort. The imbalance of only two blades also means that the turbine will need regular maintenance as materials deteriorate and efficiency decreases over time.

Three-Blade Wind Turbine:
This three-bladed horizontal axis wind turbine (HAWT) of height 50m and blade length of 30m is a much larger wind turbine. The turbine's nacelle will include an active yaw system due to the changing wind directions that are mentioned in section 2.2.1. The cost of this turbine will be greater due to the increased material and weight of the system, thus making the turbine construction and transportation more difficult. However, these turbines operate at a lower speed so there is less noise dissipating into the surrounding areas. The three blades also provide more stability and increase efficiency, 54%, however of course due to the larger structure the price will be greater. Using the equation for power output along with the average wind speed, the larger 3 blade wind turbine produces 0.50 MW, significantly more than the smaller 2 bladed turbine, however due to its large potential cost (£650K), the number of these would have to be limited. The size also restricts positioning as they aren't pleasing to the eye. Therefore, the most likely position would be out at sea or on the ridge above the resort due to the limited number that could be placed.

Darrieus Wind Turbine:
This three-bladed vertical axis design (VAWT) (Darrieus Wind Turbine, 2015) of height 14m and blade diameter of 14m, is very different to the other proposed designs as the blades are at transverse to the wind and the structure looks like an 'eggbeater'. The cost of the turbine is a lot cheaper due to less components being needed. The one main advantage is that due the vertical blades, more turbines can be placed in a smaller area and pairs of VAWTs can increase each other's performance by 15% (LUVSIDE ,2020). However, more maintenance is required and the power coefficient, 0.29, is also much lower due to only a fraction of the blades contribute to the power production. A rough estimation using the average yearly windspeed produced a power output of 0.13 MW however this could be increased when coupled with another turbine. The price would be around 70.2k so similar to the smaller horizontal 2-blade. The Darrieus turbine

seems most logical to be a part of a wind farm therefore either the on-site next to the solar panels or the off-shore site seem most probable.

2.2.4 Modelling Wind Turbines

Each wind turbine design explained in the previous section was modelled in different positions around the eco-resort site to compare energy outputs and cost to find the most logical solution. The two-bladed design wasn't considered due to its impracticality and maintenance requirements thus a 3-bladed design of same dimensions was modelled instead. The coding software Matlab was used to produced graphs on energy output from each scenario and this was possible through the function Floris (Appendix D), that evaluates each turbines power output from their respective power curves (Appendix D).

2.2.5 Turbine Layout

For the Turbine layout there were several variables to consider. The most obvious was space, the on-site farm had limited space being on top of the hill thus having a large farm wouldn't be feasible. Not only that but the number of turbines would ideally be minimised to avoid social impacts. Therefore, the offshore site would be most likely site for several turbines.

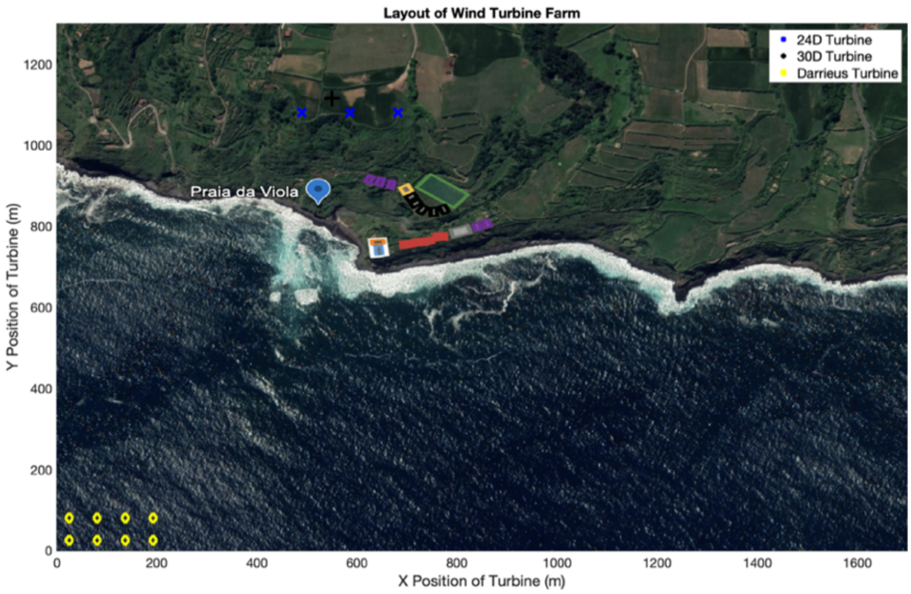

Fig. 8: The three proposed sites for the wind turbines

With the Darrieus wind turbine actually increasing power outputs by up to 15% when coupled and cost being much lower than the others, this design seemed most suitable to be a part of an offshore wind farm. Whereas the two three-bladed designs would suit the on-site location. The Matlab code was the implemented to find the number of turbines needed to produce the estimated requirement of around 400 MWh per year of energy from wind. The two proposed sites were given a different Hellman exponent due to different terrains, the higher the exponent the greater the windspeed hitting the turbine. This equation was shown in Appendix E, the on-site location was given a Hellman exponent of 0.25 due to the site being close to the coast but at the same time being influenced by the shrubs and trees surrounding it, whereas the offshore location had a much lower value of 0.10 (NASA, 1979). The turbine spacing was also heavily considered due to massive decreases in efficiency if turbines were too close. Therefore, for HAWTs the turbines were given spacing of multiples of four and seven of their respective diameters in X and Y coordinates. For VAWTs the Y coordinate spacing was reduced to four as less space is needed. Fig. 8, which shows each turbines number as well as positioning on image of Eco-Resort site. For evaluation purposes of each site the offshore wind farm is located within view of resort, obviously this would not be in view if chosen as wind source.

As shown in the Fig 8 above, to meet the suggested the annual energy output, one 30m diameter turbine was sufficient. On the other hand, three 24m diameter turbines are required with these spread along the X-axis due the spacing along the Y-axis being too large. In the bottom left, the proposed offshore site can be seen with eight Darrieus turbines working in tandem to supply energy to the resort.

2.2.6 Expected Power

The power output was produced through the use of the function of Floris, which was validated in Appendix D, using the average windspeeds through each month the power output was calculated. The Fig 9a below shows you the average power output per month of each location and turbine. Shown in Fig. 9(b) below, the singular 30m diameter wind turbine placed at the top of the hill on the back of the resort produces the highest power output per month. However, the 24m diameter produces more power during the months between June and September due to smaller turbine being more efficient with the slower average windspeeds.

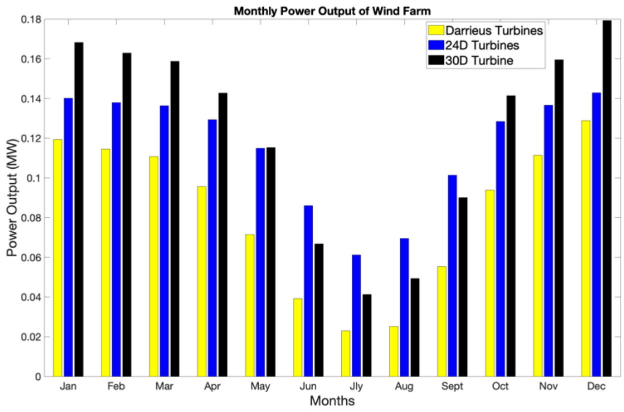

Fig. 9(a): Monthly power output of each turbine site

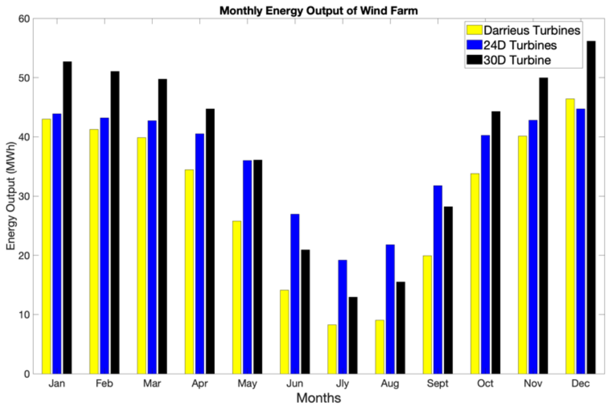

Fig. 9(b): Monthly energy output of each turbine site

This isn't a problem, however, due to solar power (refer to section 2.1.6) producing its highest power outputs during these months. From this Fig. it is also clear that the Darrieus wind turbines are not the logical solution as the power outputs are lower than both the other options. To find the energy produced per month, simply the power is multiplied by hours in a day and days in a month. Then the capacity factor (Center for sustainable systems, 2023) which is commonly around 40% (Energy Transition, 2023) for wind turbines, found by dividing maximum capacity by the average power output, this can be lower or higher. With the time and capacity now factored the energy output in MWh are produced below in Fig 9b.

As shown in Fig 9b the energy output of the 30m diameter turbine is the greatest reaching the goal of 450MWh whilst only needing one turbine, whereas both the 24m diameter turbine as well as the Darrieus turbine both fall a little short whilst needing a greater number of turbines. Obviously both the smaller turbines could have their energy output increased by expanding the farms however this will incur in greater costs this is further examined in the next section 4.2.8.

2.2.7 Construction and Maintenance cost

The overall lifetime of a typical wind-turbine is around 20-25 years. With 2 regular checks a year on all mechanical and electrical components being completed, to avoid any mechanical or electrical failures.

When proposing the idea of wind energy powering the ECO-resort this report has listed three different ways of generating this energy. However, how feasible each suggestion must be addressed. Thus, the offshore wind farm can be dismissed due to the large costs The construction and maintenance costs for eight offshore 14-meter vertical wind turbines involve various factors. Initial construction expenses can be given a rough estimation of €81.4K totalling at €650K when including all the turbines (Weather Guard, 2023). Foundation types, tailored to the specific water depth at the installation site, are a crucial consideration. Installation logistics, such as transportation and offshore assembly, contribute to upfront costs, as does the necessary electrical infrastructure for grid connection. Maintenance costs encompass ongoing expenses related to offshore access and transportation, the impact of challenging marine weather conditions on maintenance frequency and complexity, the implementation of advanced monitoring systems for predictive maintenance, and the employment of skilled personnel for routine checks and repairs. Additionally, factors like regulatory compliance, adherence to environmental standards, and insurance costs further contribute to the overall financial considerations of the offshore wind project.

Therefore, for an ECO-resort that uses wind energy as a back-up energy source it really isn't feasible to have an offshore wind farm. Looking at the proposed suggestion for onshore wind farm the three 24m diameter wind turbine would incur a cost of €241K each totalling at €731K, which is €23K cheaper than the 30m diameter turbine (€754K) (NREL, 2021), but due to there being 2 extra turbines the maintenance required will be much greater as well as construction costs. Having only one turbine keeps the carbon offset low due to less materials used and transportation costs will be much lower. The location as well makes it much easier to connect to the battery and the ECO-resort grid as it is only roughly 250m away from the battery site.

2.3 Geothermal Energy

Geothermal power is an extremely useful renewable energy source which can generate electricity and provide heating by utilising heat from the Earth. In the Azores, geothermal energy is already recognised as a significant contributor to the ongoing transition away from environmentally harmful energy sources, such as fossil fuels. There are four decades of geothermal energy experience in the Azores and there is a high contribution of up to 44% of power generation on the Sao Miguel Island (Franco, 2019). During times of low energy production from wind and solar, the aim is to consume energy from the grid in the form of geothermal.

Development of geothermal projects on Sao Miguel began in the 1970s, with the main focus on the Ribeira Grande field. This site is located in the north flank of Fogo Volcano which is the largest out of three active (dormant) central volcanoes on the island (Franco, 2019). Over the last 40 years, this field has shown promising results due to the stepwise approach that was followed, as it enabled researchers to learn from previous mistakes and maximise capacity. The source of the geothermal system is a 245°C two-phase liquid dominated reservoir, this has been exploited through relatively shallow wells ranging from 1-1.5km in depth (Franco, 2019). The field comprises of two geothermal power plants named Ribeira Grande and Pico Vermelho, with a net generation capacity of 23MW (Franco *et al.*, 2021).

2.3.1 Process of energy production

Both power plants utilise ORC (organic Rankine cycle) technology, the Pico Vermelho plant had an initial generation capacity of 3 MW which was later dismantled and replaced with a 10MW ORC binary plant in 2005/2006 (Franco, 2019). Whereas for the Ribeira Grande plant it was developed in two stages, an initial 5MW in 1994 which was further increased to 13MW in 1998 (Franco, 2019).

Pico Vermelho Plant:
This plant was designed as part of contract by ORMAT for EDA RENOVAVEIS (main renewable power generation company of the Azores). The binary cycle plant composes of a turbo generator as well as an axial turbine. In this system a two-phase process occurs, the working fluid is n-pentane, whereas the sources of heat are brine and saturated geothermal steam (Franco, 2019). The process begins with tapping into the resource with 'production' wells of up to 1km in depth. The geothermal fluid of Fogo Volcano is a two-phase source and has a low enthalpy (900-1100 kJ/kg) (Franco, 2021). These artesian wells then bring the geothermal fluid to the surface after which it enters a separator, resulting in roughly 78% brine and 22% steam (Kaplan et al., 2007). ORMAT has developed a two-phase type ORMAT® ENERGY CONVERTER (OEC) to efficiently utilise this geothermal resource. The isolated steam moves to the plant in a separate pipeline to the brine, this steam is then fed to the power plant shell and heat exchanger (two steam evaporators) where it vapourises the working fluid (n-pentane).

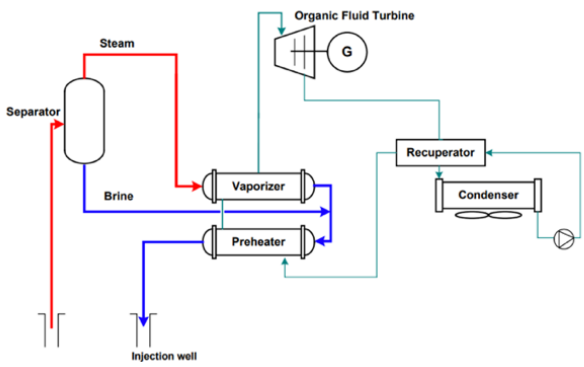

Fig. 10: Binary cycle schematic. Adapted from (Kaplan, 2022)

This transfer of heat to the working fluid causes the geothermal steam to condense. It should be noted that at this stage, the non-condensable gases are expelled into the atmosphere through a discharge valve (Rangel, 2020). The mixture of condensed steam and brine are then used in another heat exchanger (two preheaters) where they heat the working fluid. After this heat transfer, the geothermal fluid is reinjected back into the reservoir at 87°C to prevent silica scaling (Franco, 2019).

From the point of view of the working fluid, four centrifugal feed pumps raise its pressure and drives it from the condenser hot wells to the recuperator. Here it undergoes an initial heating by the n-pentane vapour stream from the turbine outlet (Franco, 2019). The fluid then moves to the preheater, participating in heat exchange process with a mixture (described in the previous paragraph) until saturation. The fluid is then carried to the evaporator where boiling occurs (see previous paragraph). Finally, the vapourised n-pentane is then driven to a turbine where it expands and turns it. The kinetic energy from the flow is then converted to mechanical energy, therefore rotating the generator shaft and producing electrical energy (using an alternator) (Franco, 2019). The working fluid then moves back to the recuperator and then a condenser. Condensation then occurs through air cooling; the remaining heat is then released into the atmosphere before restarting a new cycle. Fig. 10 illustrates the various components involved.

Ribeira Grande Plant:
The geothermal system for the Ribeira Grande plant is quite similar to that of Pico Vermelho (both binary cycle) and a detailed explanation is provided in the Pico Vermelho section. There are small differences however such as the location, number of production and injection wells. In addition, the geothermal fluid of Ribeira Grande is sodium-chloride water (Franco, 2021).

2.3.2 Results and Discussion

At the stage of design, the generation capacity of Pico Vermelho was 10 MW, however some of its production wells turned out to be highly prolific, resulting in the productivity being greater than forecasted. The ambient temperature of the air condenser cooler selected during design was 22°C, due to the average ambient temperature in the Pico Vermelho area being less than 20°C, the performance of the generation equipment is also higher than initially predicted (Franco, 2019). These factors resulted the average power output of the plant throughout its production history being 11.5 MW, in fact, 3 out of the 5 production wells are alone enough to meet the plant's capacity (Franco, 2019).

Moreover, the reserve power capacity of the system further allows for increased performance, the ORC unit has the capability to maximise the excess geothermal fluid provided by the producers (Franco, 2021). In 2022, the plant produced 90.5 GWh, with an excellent capacity factor of 103.3%. Table 2 (EDA, 2022) summarises the key output and Fig. 11(a) depicts the monthly energy output and capacity factor. The estimated availability was 90.5%, it should be noted that, the smaller energy output in January of 2022 was due to an alternator damage at the end of 2021, leading to a large period of unavailability (EDA, 2022).

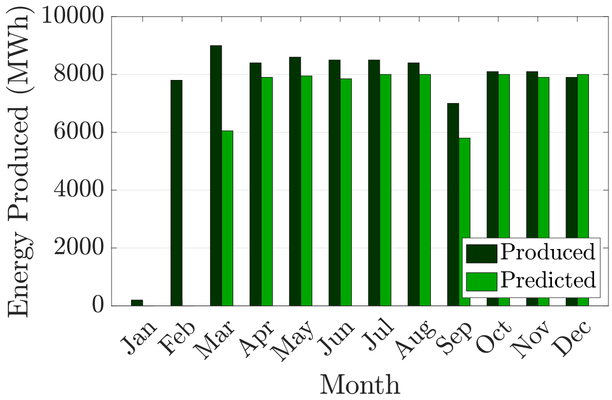

Fig. 11(a): Pico Vermelho monthly energy output.

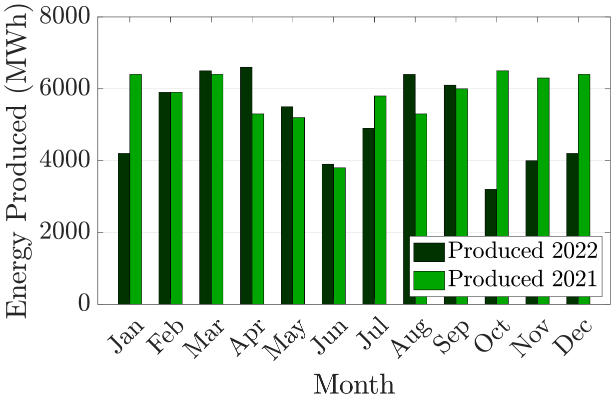

Fig. 11(b): Ribeira Grande monthly energy output.

The Ribeiro Grande plant produced 62.9 GWh in 2022 (EDA, 2022), though this was lower compared to previous years due to scheduled maintenance as well as inspections of the injection wells. This was one of the factors causing the lower availability of 65.9%, whereas the capacity factor was 55.2%. A summary of the key results as well as the monthly power output are provided above in Fig. 11(b) and below in Table 3.

Table 2: Production parameters at the Pico Vermelho plant. Adapted from (EDA, 2022).

Parameter	Unit	2022		2021
		Predicted	Actual	Actual
Energy Produced	GWh	75.6	90.5	68.03
Average Power	MW	10.9	10.3	7.8
Availability	%	78.9	90.5	66.6
Load Factor	%	86.3	103.3	78.0

Table 3: Production parameters at the Ribeira Grande plant

Parameter	Unit	2022		2021
		Predicted	Actual	Actual
Energy Produced	GWh	69.3	62.9	64.5
Average Power	MW	7.9	7.2	7.4
Availability	%	74.3	65.9	64.1
Load Factor	%	60.8	55.2	56.7

Some of the challenges posed in the Ribeira Grande field include locating an adequate reinjection location of the fluid in the northern sector and scaling (Franco, 2021). Scaling occurs when the minerals present in the geothermal fluid precipitate and form deposits. It constitutes a major problem as these deposits form on equipment such as pipelines and heat exchangers, thereby reducing flow and heat exchange, potentially reducing the overall system efficiency and productivity (Boch et al., 2017). For the Ribeira Grande and Pico Vermelho plants silica scaling is the most common and this risk was minimised by diluting the silica concentration in the brine (Franco, 2021).

2.3.3 Conclusion

Geothermal energy is vital in the Azores, and even with it currently supplying 44% of the electricity needs to the Sao Miguel island, there are still further plans to expand it. There are on-going plans to increase the generation capacity of the Pico Vermelho site from 10 MW to 20 MW (Cariaga, 2023) with a new geothermal plant. The feasibility study already shows there is enough of the geothermal resource to support this increase (Cariaga, 2023), this clearly supports our aim of using carbon negative energy resources and the expected completion time of this project is 2025. In addition, geothermal systems are commonly designed to fulfil the base of the load diagram, as it is always constantly on. Though, the lowered demand during off peak hours may hinder this additional capacity that can be installed (Franco, 2019). For example, thermal plants provide grid forming capabilities that ensure energy stability. Hence, the incorporation of added geothermal production may be dependent on the ability of the system to perform the same grid forming capabilities as other power generation sources (Franco, 2019). Some suggestions have been made such as using a similar method of that used in the Puna Ventura plant, Hawaii, where the units of the binary system have the ability to ramp up and down according to the load needs (Franco, 2019). Conversely, the implementation of an improved energy storage system can be considered and it has recently been achieved on two islands through Siemens and Fluence's 15-megawatt battery-based storage (Siemens, 2023). Lastly, it should be made clear once again that this energy resource will not be produced on site, but imported from the grid. Our hope is to engage in a sort of renewable energy buying scheme with EDA that will allow us to solely get geothermal, this may be in the form of a Power Purchase Agreement (PPA).

2.4 Combined Energy

Fig. 12 illustrates the complete breakdown of energy sources contribution to the total energy consumption of the resort. During months where solar energy and wind are not producing sufficient energy, geothermal energy from the grid is used. During months where excess energy is produced, it is exported back to the grid. More on the systems of this are discussed in the following section. 97.76MWh of Geothermal energy is consumed by the resort from the grid. Over the year the energy systems produce 105.02 MWh of excess energy. Therefore, overall 7.26MWh of electricity is being given back to the grid every year.

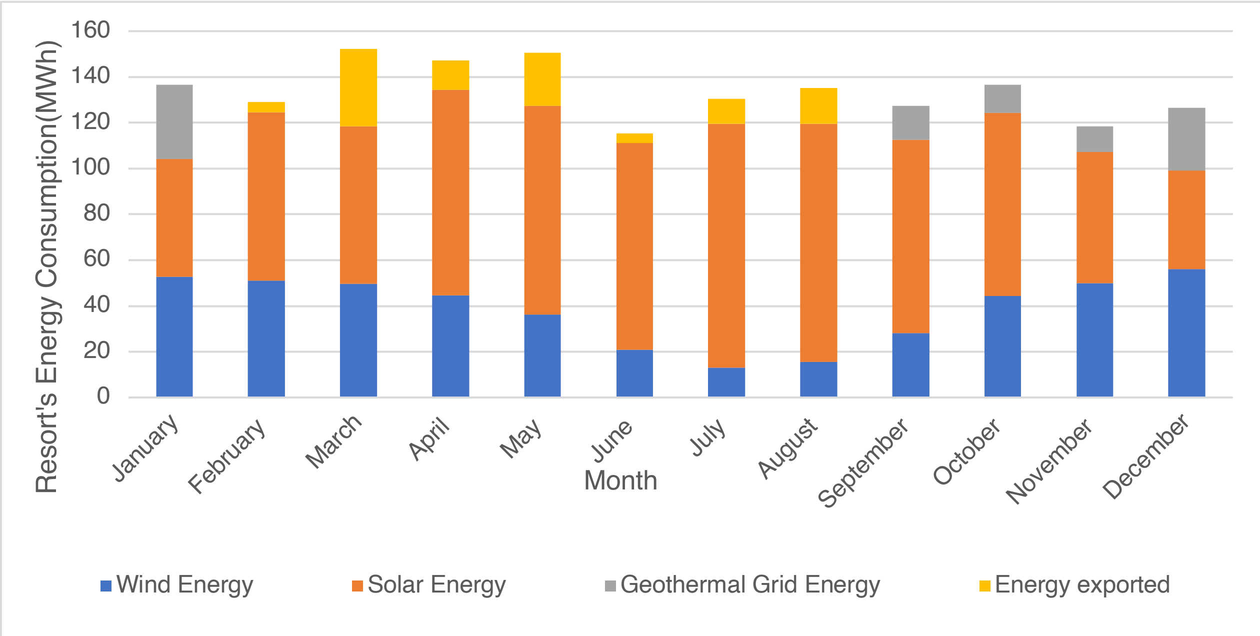

Fig. 12: Monthly energy source contribution towards the energy consumption

3 Storage and Systems

This section addresses the strategic management and distribution of generated energy throughout the resort. The focus commences with proposing a viable solution to handle any excess energy produced. Following this, the section elaborates on the intricate details of how the energy produced is effectively distributed on site.

3.1 Energy Storage

3.1.1 Summary

The ECO Resort's strategic initiative for sustainable energy storage results in the selection of repurposed EV batteries, balancing cost, efficiency, and environmental sustainability. Comparative analysis reveals battery storage as more suitable for our operational context than hydrogen storage, with used EV batteries being particularly favoured for their lower cost and reduced ecological footprint. The investment of approximately $1.7 million into the battery storage system ensures the resort's energy reliability and aligns with our eco-friendly objectives, while the modular system design facilitates future technological integration and expansion.

3.1.2 Introduction

In our search for sustainable operations, the energy storage system at ECO Resort is key. This section compares battery storage systems, including used EV batteries, alongside hydrogen storage, evaluating their fit for our energy needs. Our goal is to implement a solution that is eco-friendly, efficient, and reliable. We're considering the advantages and practicality of each system, with a focus on the environmental and economic benefits of repurposing EV batteries for stationary energy storage at our resort.

3.1.3 Comparative Analysis of Energy Storage Systems

Energy storage is critical for balancing demand and supply, ensuring reliability and optimising the use of renewable sources. Our comparative analysis considers two primary technologies: battery storage and hydrogen storage.

Efficiency: Batteries typically exhibit 80-90% round-trip energy efficiency, meaning most stored energy is available for use (Meister, P., Jia, H., Li, J., Kloepsch, R., Winter, M. and Placke, T. (2016)). In contrast, hydrogen systems have a lower efficiency of about 35-50% due to losses in electrolysis, storage, and conversion back to electricity.

Cost: While batteries have high initial costs, their prices have been decreasing, and they offer cost-effectiveness varying with technology and scale (Curry, C. (2017)). Hydrogen storage involves higher initial costs for electrolysers, storage infrastructure, and fuel cells, potentially becoming more cost-effective at larger scales or for long-term applications.

Energy Density: Batteries have lower energy density compared to hydrogen, leading to a larger physical footprint for equivalent energy storage (Cao, W., Zhang, J. and Li, H. (2020)). Hydrogen's high energy density is ideal for long-term and large-scale storage where space is less constrained.

Scalability and Flexibility: Battery systems offer scalability within limits and are easier to integrate with existing power systems. Hydrogen storage is highly scalable, suitable for larger and longer-duration storage, and beneficial for seasonal storage.

Lifecycle and Degradation: Batteries undergo degradation over time with typical lifespans of 5-15 years, depending on technology (Dunn, J., Kendall, A. and Slattery, M. (2022)). Hydrogen systems show less degradation over time but require more data for long-term performance assessment.

Environmental Impact: The manufacturing and disposal of batteries have environmental implications, although recycling processes are evolving (Meshram, P., Mishra, A., Abhilash and Sahu, R. (2020)). Hydrogen has a minimal environmental impact when produced from renewable sources, but the production of associated technologies also has environmental considerations.

Operational Aspects: Batteries generally require minimal maintenance and are operationally straightforward. Hydrogen involves more complex operation and higher maintenance, particularly due to high-pressure storage requirements.

Application Suitability: Batteries are more suitable for short to medium-term storage and load balancing, while hydrogen is better for long-term storage, especially in scenarios with excess renewable energy production.

Market Maturity: The battery market is mature with a diverse range of products and established supply chains. In contrast, hydrogen storage is an emerging market that is rapidly developing but may offer less variety and established infrastructure.

In conclusion, battery storage emerges as more appropriate for our resort, focusing on efficiency and compact storage for short to medium-term energy backup. Hydrogen storage could be preferable for large-scale, long-term storage, particularly when maximising the use of excess renewable energy. The final choice will depend on specific factors such as budget, space availability, environmental priorities, and our resort's long-term energy strategy.

3.1.4 Detailed Analysis of Selected Battery Systems

After a comprehensive review, we have narrowed down our focus to four battery systems: BSLBATT, RJ Lithium, Symtech Solar Megatron, and Recycled EV batteries. These systems were evaluated based on their capacity, cycle life, operational aspects, and environmental impact.

BSLBATT Battery System: Offers a modular design with a capacity that can be scaled according to need. However, its cycle life is shorter than the RJ Lithium, and it requires more frequent maintenance.

RJ Lithium 100 kWh Battery Energy Storage System: Stands out for its longer cycle life and robust warranty. It is particularly compatible with our resort's renewable energy sources, offering uninterrupted power supply (UPS) functionality. This system can reliably support the resort's energy needs during peak hours and emergencies.
Symtech Solar Megatron Battery System: Known for its high energy density and environmentally friendly design. However, its higher cost and the complexity of integration with existing renewable sources make it less favourable for our current needs.

Recycled EV Batteries: Present a sustainable and cost-effective option with a good balance of capacity and cycle life suitable for stationary storage, despite their prior use in vehicles (Abdelbaky, M., Peeters, J.R. and Dewulf, W. (2021)).

Among these, the used EV batteries stand out as the preferred option, offering a harmonious balance of cost, efficiency, and environmental sustainability, making them the most suitable choice for our eco-resorts energy storage needs.

3.1.5 Calculation of Battery Requirements

In determining the number of used EV batteries needed to support the resort's energy infrastructure, we've meticulously analysed daily energy consumption, peak load demands, and the essential requirements for emergency backup. Our findings suggest that each used 75 kWh EV battery, with an adjusted usable capacity of 50 kWh to account for health depreciation, would necessitate a fleet of 155 batteries to ensure continuous power over a span of three days (Casals, L.C., Amante García, B. and Canal, C. (2019)). To further safeguard against possible inefficiencies and unexpected surges in energy usage, we've prudently increased this estimate to a total of 175 batteries.

From a financial perspective, while new batteries are typically priced at approximately €130 per kWh, used EV batteries present a substantial cost reduction, falling between 30-70%. By adopting a conservative approach, we've estimated a cost-saving of 35%, setting the price of used batteries at around €85 per kWh. Consequently, procuring 175 batteries, each with a capacity of 75 kWh, would culminate in an investment close to €1,106,250. This strategic expenditure is a testament to our unwavering dedication to sustainability and operational excellence. By leveraging robust energy storage solutions, we ensure the fulfilment of our regular operational needs as well as comprehensive emergency preparedness.

To complement our battery array, the associated supporting electronics, which encompass around 30% of the battery pack cost, coupled with the installation of 300 metres of cabling, are projected to incur an expense of €100,000 (Mongird, K., Viswanathan, V., Balducci, P., Alam, J., Fotedar, V., Koritarov, V. and Hadjerioua, B. (2020)). Additional installation costs, estimated to be about 15% of the battery investment, will also be accounted for. This brings our total setup expenditure to approximately €1,700,000—a calculated investment in our resort's energy autonomy.

Maintenance, an integral component of system longevity and performance, will be conducted quarterly. These routine check-ups will include inspecting connections, monitoring battery health, and updating software systems. Furthermore, a yearly in-depth review will pinpoint any significant maintenance needs. We have allocated an estimated annual maintenance budget of €100,000 to cover labour and potential component replacements, ensuring our energy storage system remains at the pinnacle of efficiency and reliability.

3.1.6 Optimal Placement of Battery Storage System

The placement of the battery storage system is crucial for both safety and efficiency. Factors considered include proximity to energy sources, accessibility for maintenance, and risk management. Our analysis recommends situating the battery system near the solar power hub to minimise transmission losses and facilitate easier monitoring and maintenance. This location also aligns with safety protocols, allowing for isolated and secure storage away from guest areas. Adequate ventilation and protection from environmental elements are also integrated into the design to ensure the longevity and safety of the system.

Potential risks include system failure, operational downtime, and safety hazards. Mitigation strategies will involve regular maintenance checks, the integration of a robust monitoring system to predict failures before they occur, and strict adherence to safety protocols. An emergency response plan will be developed to address any immediate risks posed by the storage system.

Compliance with local energy storage regulations will be verified through consultation with relevant authorities. The system will be designed to meet all safety and environmental standards, with documentation prepared for regular audits. Compliance will also extend to installation and operational procedures.

3.1.7 Conclusion

The initial investment in the battery storage system is estimated at €1,700,000, with operational costs averaging €100,000 per annum. As the resort grows and technology evolves, the energy storage system is designed to be modular for easy expansion. Future battery technology advancements will be monitored, and the system's design allows for straightforward integration of new battery modules or the replacement of existing ones to increase capacity or efficiency.

Our comprehensive analysis underscores the Used EV Battery storage system as the optimal choice for our ECO Resort's energy storage needs. This system aligns with our commitment to sustainability, offering high efficiency, reliability, and compatibility with renewable energy sources. The strategic placement of the battery storage further enhances safety and operational efficiency. Adopting this solution represents a significant step towards achieving our eco-friendly goals, ensuring a reliable and efficient energy supply for the resort.

3.2 Energy Sources

3.2.1 Geothermal

The geothermal energy supplied to the resort will be distributed from the main grid. This process can be described by two sages: power transmission and distribution. The geothermal power plants produce a three-phase alternating current (AC) power, this power moves from the generator to the transmission substation where the voltage is increased. This step up in voltage allows for a reduced current thereby minimising the power loss in the transmission line, this is important especially over long distances. In addition, thinner electrical lines can be used for lower currents, this reduces potential construction costs (IEP, 2023).

For the power to be used by the resort guests, it needs to be 'distributed' at a lower voltage, power distribution is this conversion of high voltage electricity to a lower voltage (IEC, 2023). The transition from transmission to distribution happens in a power substation, involving three aspects, stepping down the voltage with a transformer, distribution of the power in various directions and disconnection using circuit breakers (Brain & Roos, 2023). The power leaves the transformer and enters the distribution bus where it is distributed in multiple directions. Due to it being an island, the Azores' distribution lines are underground. Using what is known as a distribution transformer, the voltage is finally stepped down to the level that can be used by the resort. Distribution transformers may be attached to a pole, mounted on the ground or underground (Dreger, 2014). On the island of San Miguel, the transmission network has a high connection voltage of 60kV, followed by the distribution network that consists of lines with medium connection voltages of 30kV and 10kV (Melo, 2020). This voltage is finally distributed to consumers at 0.4kV (Melo, 2020). Similar to the European continental system, the network is operated at a frequency of 50 Hz (Cross-Call, 2023).

3.2.2 Wind Energy

Wind turbines harness wind energy to generate electricity through a series of interconnected components. As the wind blows, it causes the rotor blades to rotate around the central hub. The rotor connected to the shaft, which, in turn, is linked to the gearbox, which increases the rotational speed for electricity generation. This high-speed shaft connects to a generator, where electromagnetic induction occurs as the rotating magnetic field passes through conductive coils. This process, based on Faraday's law, induces an electromotive force, converting mechanical energy into electrical energy. The generator produces alternating current (AC), typically three-phase AC, suitable for integration into the micro-grid.

3.2.3 Solar Energy

Solar energy uses an inverter (Renewableshop.co.uk, 2023) to convert the current from DC to AC as outlined in Section 2.1.6.

3.3 Microgrids

A vision of the resort's primary energy sources has been outlined, nevertheless, a key question remains: how will these sources synergize and operate cohesively? Our approach focuses on harnessing the power produced by seamlessly integrating these sources into a cutting edge microgrid (MG) system. A microgrid can be described as a self-sustaining energy system that generates and distributes its own power while integrating energy storage systems (Wood, 2023). Specifically, the MG for the resort can be classified as a renewable hybrid system (AC and DC) (Udden et al., 2023). Microgrids, being localised, enable the mitigation of power losses over extended distances, thereby offering distinct advantages. They can also connect to the main grid in 'grid-connected mode' or operate independently from it in 'island mode'. Microgrids can also be controlled, allowing for optimal performance.

3.3.1 Features and Layout

Highlighting some of the hybrid system's features, it has all the benefits of a conventional AC/DC systems, for example, there are smaller power conversion losses due to fewer conversion stages. This means there is increased efficiency, lower cost and a smaller sized system (Abbasi et al., 2023). The MG will consist of a single wind turbine and a solar farm at different locations around the site as described in. The maximum power output of the wind turbine is 300kW, whereas the solar PV panels can produce up to 787.2kW. As outlined earlier, energy storage will also be incorporated in the design in the form of batteries, they play a crucial role by providing power during times of fluctuations in energy generation.

A the has various components which can be summarised as follows. The **load** which include AC and DC loads from the villas, restaurants and spa. The **energy storage system** which are the batteries, **DERs** (distributed energy resources) which can be classified into the AC source (wind farm) and the DC source (PV system). Furthermore, there are **power converters** to aid in transferring energy between the AC and DC networks. Connecting the MG to the main grid on Sao Miguel involves establishing a link between them via a Point of Common Coupling (PCC).

3.3.2 Control

As for the control of the microgrid, this is at the heart of managing and optimising the generation, distribution, and consumption of energy within the microgrid and will help minimise disruption to resort guests. The MG will feature a centralised system in which a single controller will manage the entire system. The hierarchal control of the system can be divided into three levels namely, primary, secondary and tertiary control.

The role of *primary control* is to maintain the MG's voltage and frequency, facilitating improved power sharing among distributed energy resources (DERs). It boasts the fastest response time among the three in achieving its objectives. For example, during instances of rapid drop in solar power output, the primary system can detect this and perhaps adjust the output of the battery storage to compensate. In addition, it helps regulate the frequency and voltage during times of power demand fluctuations.

Secondary control has a slower response than primary (Abbasi et al., 2023), it is also known as an energy management system, it mitigates the deviations in voltage and frequency from primary control. The slow response is attributed to its role in regulating the set points, the scheme utilises complex/advanced algorithms which are based on factors such as power losses and economic revenue. The aim is to have the grid in islanded mode most of the time, in this mode the secondary control is the highest level of the control system.

Finally, there is *tertiary control* which has the longest time scale of the three, in grid-connected mode, it manages the import and export of power to the main grid. Additionally, it is important to highlight the influential role that artificial intelligence can wield in the MG system, as the proposed MG seeks to harness and leverage certain aspects of its capabilities. Combining AI techniques with the existing hierarchal control scheme can increase the scheme's effectiveness (Borghese, 2023) in turn increasing efficiency and cost effectiveness. The aim is to have AI algorithms used in tandem with the control scheme. For example on the secondary level, other inputs may be added such as weather forecasts or energy tariff prices to boost microgrid performance, therefore surpassing conventional systems that rely on model predictivity. Integrating AI will not only allow the use of real time data, but the model will have the ability to learn from the MG's long-term patterns to further improve optimisation.

3.3.3 Benefits and Challenges

Microgrids will potentially play an integral role in achieving our objective of operating a resort fully powered by renewables and it has various strong attributes, the limitations one may face during deployment also have to be recognised however. These are both outlined below:

Benefits:
Renewable integration: These again play a huge role in contributing to significantly reducing carbon emissions by facilitating in the incorporation of renewable sources.
Continuous independent supply: In the islanded mode, the MG continuously provides energy supply from the onsite renewable sources. This means that the resort's supply will remain unaffected during any periods of disruptions to Sao Miguel's main grid.
Grid support: MGs can facilitate the generation increase of the main grid, the resort's MG can export the excess renewable energy produced, potentially boosting economic sustainability.

Challenges:
Operation: Due to the fact that the MG can be operated in two modes, there may be discrepancies between the generation and demand, which can cause frequency and voltage issues.

Compatibility: As the MG has a variety of components, ranging from wind turbines, inverters to communication devices, their characteristics (start-up time, operational cost, etc.) vary greatly, these may lead to compatibility issues. While the MGs are extremely useful, some of its challenges need to be acknowledged in order for a successful implementation in the resort.
Load management: determining ideal values in energy regulation is often difficult,
Design: There are design issues present specifically when integrating renewables sources, in this case, wind and solar. There is difficulty in determining a proper design of the MG as it requires a thorough understanding of the energy availability, the dramatic fluctuation of these sources could make the MG unstable (Saeed, 2023).
System security/protection: Some of the problems that can cause faults range from accidental disconnections to cyber-attacks. Robust measures need to be implemented to ensure energy reliability, these may include contingency plans and emergency actions (load shedding, islanding, complete unit shutdown). Furthermore, protection devices such as fault current limiters and fast static switches will be used.

4 Impact Analysis

4.1 Wind and Solar farm impacts

Of course, when looking at constructing a wind turbine anywhere there are several important steps and considerations that must be addressed. These include: Permitting and Regulations; Environmental Impact Assessment; Community Engagement; Land Rights and Agreements. All of these will be further researched to ensure the ECO-resorts plan to construct a wind turbine.

First of all, before anything else can be done, the Isle of San Miguel's permitting laws regarding the construction of a wind turbine must be considered. Portugal seems to be keen for renewable energy sources to be constructed (WINDPOWER, 2010) with wind farms of a similar if not greater size being constructed in other areas over the last couple of years (IRENA, 2020) thus it can be assumed that there wouldn't be a huge objection for the construction. The construction of solar panels should be simpler as they will be on the main site of the resort, refer to Fig. 2, and they won't affect the landscape as much as the turbine. An Environmental Impact Assessment was also undertaken to try and mitigate any sort of problems that may be faced when implementing the turbine. This is evaluated in Table 4 shown below.

Regarding the Community engagement and Land rights, due to the previous use of the area being an abandoned water mill site, there shouldn't be too many difficulties in ensuring the rights for the land. With any landowner being compensated if they have been affected by the construction. Before construction locals will be encouraged to join a meeting with the representatives of the Eco-resort to discuss impacts and possibilities of working at the resort, thus providing jobs for the community. Any excess energy will be dissipated to the main-grid but exploring ways of transmitting to the surrounding villages and towns that may have been affected by the construction of the turbine or solar panels could be done.

Table 4: Environmental Impact Assessment.

Potential Impact	**Mitigation**
Visual Impact	Limited the number of turbines to one and location is at the top of a ridge with limited number of residents within the vicinity (nearest villages roughly 600m away). Engage with local communities to address aesthetic concerns.
Noise Impact	Only a single turbine, which is fairly large thus will not operate at high speeds so noise shouldn't be a problem. During construction of both turbine and solar farm, work hours will be in accordance to local laws.
Animal Impact	Wind turbine can cause huge impacts on birds due to difficulties in seeing the blades, thus one blade tip will be painted black. This has been proven to reduce impact on birds. Off-shore not chosen due to impacts it can have on coral-reef and ecosystem.
Cultural Heritage	Previous site was an abandoned water mill, which used to be the original source of renewable energy.

Socio-Economic Impact	Will provide jobs for the local communities to work at resort or as part of the maintenance crew for the renewable sources. Will also provide any excess energy to the surrounding villages.
Health and Safety	Implement strict safety protocols for construction workers and maintenance crew. Collaborate with local emergency services for response plans in case of unfortunate event.

4.1.1 Carbon Footprint

In 2018 it is shown that on the San Miguel Island, 49% of energy that supplies the island comes from oil and diesel, 42% from geothermal, 5% from hydroelectric and 4% from wind (EDA S. A. 2007–2018., 2018). To find the carbon offsetting, a weighted average calculation was done to find the overall g per kWh of carbon emissions of the electricity suppled from the grid. Using equation 8 below,

$$\begin{aligned} &Weighted\ Average\ of\ carbon\ footprint\ of\ grid\ electricity \\ &= (266.5 * 0.49) + (38 * 0.42) + (25 * 0.05) + (11 * 0.04) = 148.19 \end{aligned} \tag{8}$$

This value was 148.19g of CO2 per kWh of energy produced. This is the weighted average carbon footprint of the grid supplied energy. Around 44g of CO2 per kilowatt-hour is produced during the first years of operating a solar energy system Helman, C. (2021). For the solar site in the ECO-Resort the carbon offset would equal 45,980 kg for the 1,045 MWh of energy produced per year. this leads to an average reduction of around 108,878KG of CO2 production per year compared to sourcing the energy from the grid. The solar panel's carbon footprint is roughly 20 times less than the carbon output of coal-powered electricity sources. As a result, the carbon footprint will decrease as soon as solar power is installed in the resort. However, the solar panels will need to be in operation for three years to become carbon neutral, paying off their carbon debt. Then, after three years of use, the overall carbon footprint will reduce further, as the system will remain carbon neutral for the rest of its lifespan (Forbes, 2021).

Wind turbines of a life-cycle basis average just 11 grams of CO_2 emission per kWh of electricity (Ninja, 2023), therefore when the 30D turbine producing 462 MWh a year, the emissions would roughly equate to 7,062 kg of CO_2. Wind produces only 11g of CO2 per kWh of electricity produced. This means that over the year, wind energy causes a reduction of around 86,394kg of CO2 emissions when compared to energy from the grid. The breakdown of this is explained below and potential improvements are discussed to reduce this impact. The construction and manufacturing phase produces the majority of carbon footprint, with 75-85%. The steel tower makes up 30% of the carbon impact with the carbon fibre and fibre-glass blades making up 12% (Atmos, 2022).

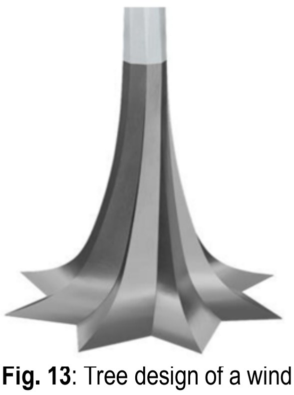

Fig. 13: Tree design of a wind turbine base.

Due to the turbine being on-shore, a concrete foundation is needed to hold the structure in place and this makes up 17% of the carbon impact. To try and reduce the impact of the turbine, different ways of providing a foundation was researched as the tower and carbon fibre are unavoidable. A Swedish design (Intelligence for Architects, 2023) was considered as they use the concept of roots in trees to hold the turbine in place as shown in Fig. 13. This would essentially cut roughly 17% of the impact with no concrete used. Swedish companies Hybrit and H2 Green Steel are investing billions to produce millions of tons of green steel, using renewable power and green hydrogen electrolysis instead of traditional methods.

They're also focusing on reducing the carbon footprint of wind and solar projects by recycling old photovoltaic panels and turbine blades (Solaris Renewables, 2023). In Italy, Sasil aims to recycle 3,500 tons of solar panels annually, while Veolia in France plans to increase its panel recycling capacity to 4,000 tons a year. Researchers at Arizona State are developing electrochemical processes to extract metals from solar cells (COOL Effect, 2021). These would all be implemented to try and reduce the carbon offset of the ECO-resort.

4.2 Battery Impact

In incorporating a Battery Energy Storage System (BESS) within the ECO-resort, meticulous planning ensures compliance, ecological preservation, and community harmony. Permitting laws within the Isle of San Miguel are favourable for renewable projects, indicating a welcoming environment for BESS integration, with less extensive landscape effects anticipated compared to wind turbines. Integrating a BESS into our ECO-resort's infrastructure requires a comprehensive understanding of both the benefits and the environmental considerations associated with battery technology, particularly lithium-ion batteries. These batteries, while offering high efficiency and energy density, also raise concerns about lithium mining's ecological footprint and the challenges associated with battery end-of-life disposal (Costa, C.M., Barbosa, J.C., Gonçalves, R., Castro, H., Campo, F.J.D. and Lanceros-Méndez, S. (2021)).

To address these issues and diminish our environmental impact, we are taking a proactive approach by utilising used lithium-ion batteries. This not only extends the useful life of these batteries but also significantly reduces the demand for new lithium extraction and battery production, with their associated environmental stresses. By repurposing these batteries, we aim to cut down on the raw material consumption and the carbon footprint generated from the production of new batteries. Moreover, our commitment to a circular economy is further demonstrated through planned partnerships with recycling programs, ensuring that the batteries are responsibly recycled at the end of their second life, thus mitigating the potential for environmental harm.

This approach reflects our broader sustainability strategy, which emphasises the reduction of waste, the extension of product lifecycles, and the responsible sourcing of materials. It aligns with global best practices in waste reduction and resource efficiency, ensuring that our resort remains at the forefront of environmental stewardship (Weterings et al., 2013).

A detailed Environmental Impact Assessment (EIA) will inform BESS design and placement to mitigate ecological disturbances. Technical analyses will ensure the BESS's compatibility with the micro-grid, enhancing energy stability and efficiency. Strategic site selection aims to balance logistical needs with the conservation of the resort's natural beauty.

Community engagement initiatives will promote understanding and support for the BESS project. Employment opportunities arising from the project will contribute to local economic growth, reinforcing the resort's socio-economic impact (rye.esmclients.com, 2021).

Visual aesthetics will be preserved through thoughtful BESS design, employing natural screening and careful placement. Operational noise will be minimised to maintain the resort's tranquillity, exceeding local noise regulations. Wildlife corridors and construction timing will protect local fauna, while cultural heritage and socio-economic upliftment will be prioritised.

Health and safety protocols will protect personnel and visitors, with emergency response plans established in collaboration with local services. A carbon footprint analysis will guide the reduction of emissions across the BESS lifecycle, with an Impact Mitigation Plan documenting strategies to minimise environmental impacts.

These measures, combined with energy education and excess energy distribution initiatives, affirm the resort's sustainability commitment. The BESS will exemplify operational excellence and stewardship, positioning the ECO-resort as a model of responsible energy management and sustainable tourism, contributing to a greener future.

5 Conclusion

This proposal presents a resort that could potentially be powered fully by renewables all year round. It has shown the possibility of reducing the resort's carbon footprint with the implementation of both solar and wind energy sources, that, during times of low energy production can be backed up by another renewable energy source – geothermal from the grid. This is evident by the reduction in carbon offset per year by roughly 180,000 kg compared to being solely reliant on the main grid. The total cost of the project is roughly €3M, which encapsulates the solar cost (€370k), the wind cost (€754k) and the battery storage cost (€1.7M), as well as smaller expenses such as geothermal grid energy and resort maintenance. By breaking down the total cost of the project, it is clear why we decided to use solar as the main source of energy due to the much cheaper price per MWh compared to wind. However, having these both work in tandem provides the perfect energy production due to how they complement each other. One aspect that could be looked into is dissipating any excess energy to the surrounding villages, rather than sending back to the main grid, to appease the locals who might've been affected by the construction. Perhaps through the extension of the proposed microgrid in the form of a 'community microgrid'.

6 References

Abbasi, M., Abbasi, E., Li, L., Aguilera, R.P., Lu, D. and Wang, F., 2023. Review on the microgrid concept, structures, components, communication systems, and control methods. *Energies*, *16*(1), p.484

Abdelbaky, M., Peeters, J.R. and Dewulf, W. (2021). On the influence of second use, future battery technologies, and battery lifetime on the maximum recycled content of future electric vehicle batteries in Europe. *Waste Management*, 125, pp.1–9. doi:https://doi.org/10.1016/j.wasman.2021.02.032.

ATMOS. (2022). *Carbon Footprint of Wind Turbines*. [online] Available at: https://www.joinatmos.com/blog/carbon-footprint-of-wind-turbines [Accessed 5 Dec. 2023].

Blewett, D. (2023). *Wind Turbine Cost: Worth The Million-Dollar Price in 2020?* [online] Weather Guard Lightning Tech. Available at: https://weatherguardwind.com/how-much-does-wind-turbine-cost-worth-it/ [Accessed 23 Nov. 2023].

Boch, R., Leis, A., Haslinger, E., Goldbrunner, J.E., Mittermayr, F., Fröschl, H., Hippler, D. and Dietzel, M., 2017. Scale-fragment formation impairing geothermal energy production: interacting H 2 S corrosion and CaCO 3 crystal growth. *Geothermal energy*, *5*, pp.1-19.

Borghese, F. (2023) *How AI powers today's advanced microgrids*, *Schneider Electric*. Available at: https://perspectives.se.com/blog-stream/how-ai-powers-today-s-advanced-microgrids (Accessed: 4 December 2023).

Brain, M. and Roos, D. (2023) *How power grids work*, *HowStuffWorks Science*. Available at: https://science.howstuffworks.com/environmental/energy/power7.htm (Accessed: 20 November 2023).

Cao, W., Zhang, J. and Li, H. (2020). Batteries with high theoretical energy densities. *Energy Storage Materials*, [online] 26, pp.46–55. doi:https://doi.org/10.1016/j.ensm.2019.12.024.

Cariaga, C. (2023) *Tender – construction of Pico Vermelho Geothermal Power Plant, Portugal*, *Think GeoEnergy - Geothermal Energy News*. Available at: https://www.thinkgeoenergy.com/tender-construction-of-pico-vermelho-geothermal-power-plant-portugal/ (Accessed: 29 November 2023).

Casals, L.C., Amante García, B. and Canal, C. (2019). Second life batteries lifespan: Rest of useful life and environmental analysis. *Journal of Environmental Management*, 232, pp.354–363. doi:https://doi.org/10.1016/j.jenvman.2018.11.046.

Center for Sustainable Systems. (2023). *Wind Energy Factsheet*. [online] Available at: https://css.umich.edu/publications/factsheets/energy/wind-energy-factsheet#:~:text=The%20capacity%20factor%20of%20a [Accessed 30 Nov. 2023].

Cool Effect. (2021). *Carbon Footprint of Solar Panel Manufacturing*. [online] Available at: https://www.cooleffect.org/solar-carbon-footprint [Accessed 5 Dec. 2023].

Costa, C.M., Barbosa, J.C., Gonçalves, R., Castro, H., Campo, F.J.D. and Lanceros-Méndez, S. (2021). Recycling and environmental issues of lithium-ion batteries: Advances, challenges and opportunities. *Energy Storage Materials*, [online] 37, pp.433–465. doi:https://doi.org/10.1016/j.ensm.2021.02.032.

Cross-Call, D.F., (2013). *Matching energy storage to small island electricity systems: a case study of the Azores* (Doctoral dissertation, Massachusetts Institute of Technology).

CSI Solar Co., Ltd. (2023). *HiKu6 Mono PERC*. [online] Available at: https://cdn.shopify.com/s/files/1/0257/3103/9284/files/CS-Datasheet-HiKu6_CS6R-MS_v1.9C25_EN-25-years-product-warranty_1.pdf?v=1679588966 [Accessed 5 Dec. 2023].

Curry, C. (2017). *Lithium-ion Battery Costs and Market Squeezed margins seek technology improvements & new business models*. [online] Available at: https://enerjiye.com/wp-content/uploads/2021/07/battery-market.pdf.

Dobos, A. (2014). *PVWatts Version 5 Manual*. [online] Available at: https://pvwatts.nrel.gov/downloads/pvwattsv5.pdf.

Dreger, S. (2014) *How is power stepped down?*, *Energized by Edison*. Available at: https://energized.edison.com/stories/how-is-power-stepped-down#:~:text=Before%20this%20power%20can%20be,change%20one%20voltage%20to%20another. (Accessed: 1 December 2023).

Dunn, J., Kendall, A. and Slattery, M. (2022). Electric vehicle lithium-ion battery recycled content standards for the US – targets, costs, and environmental impacts. *Resources, Conservation and Recycling*, 185, p.106488. doi:https://doi.org/10.1016/j.resconrec.2022.106488.

EDA (2022) RELATÓRIO E CONTAS 2022. Available at: https://www.eda.pt/GrupoEda/Paginas/FichaEmpresaEDARENOVAVEIS.aspx

EDA S. A. 2007–2018. (2018)Annual Report and Accounts. https://www.eda.pt/GrupoEda/Paginas/FichaEmpresaEDARENOVAVEIS.aspx

Energy Transition. (2023). *Capacity factor – Energy Transition* . [online] Available at: https://wiki.energytransition.org/wiki/capacity-factor/#:~:text=In%20practice%2C%20an%20onshore%20wind [Accessed 30 Nov. 2023].

EU Science Hub. (n.d.). *PVGIS typical meteorological year (TMY) generator*. [online] Available at: https://joint-research-centre.ec.europa.eu/photovoltaic-geographical-information-system-pvgis/pvgis-tools/pvgis-typical-meteorological-year-tmy-generator_en.

F. Holmgren, W., W. Hansen, C. and A. Mikofski, M. (2018). pvlib python: a python package for modeling solar energy systems. *Journal of Open Source Software*, 3(29), p.884. doi:https://doi.org/10.21105/joss.00884.

Faiman, D. (2008). Assessing the outdoor operating temperature of photovoltaic modules. *Progress in Photovoltaics: Research and Applications*, 16(4), pp.307–315. doi:https://doi.org/10.1002/pip.813.

Franco et al. (2021). Forty Years of Power Generation at the Ribeira Grande Geothermal Field, Azores. In Proceedings World Geothermal Congress 2020.

Franco, A., Vieira, N., Ponte, C. and Rangel, G., (2019). A decade of geothermal commercial production from the Pico Vermelho power plant, São Miguel Island, Azores. In *European Geothermal Congress 2019, Den Haag, The Netherlands*.

Franco: The role of geothermal in the Energy Transition in the Azores, Portugal (2019) *Eurogeologists*. Available at: https://eurogeologists.eu/franco-the-role-of-geothermal-in-the-energy-transition-in-the-azores-portugal/ (Accessed: 29 November 2023).

Helman, C. (2021). *How Green Is Wind Power, Really? A New Report Tallies Up The Carbon Cost Of Renewables*. [online] Forbes. Available at: https://www.forbes.com/sites/christopherhelman/2021/04/28/how-green-is-wind-power-really-a-new-report-tallies-up-the-carbon-cost-of-renewables/?sh=65cb80ed73cd [Accessed 5 Dec. 2023].

I.T.S Technologies. (2023a). *410W Canadian Solar Super High Power solar panel next day delivery – ITS Technologies*. [online] Available at: https://www.itstechnologies.shop/collections/solar-panels-buy-online/products/410w-canadian-solar-super-high-power-mono-perc-hiku-with-mc4-evo2-solar-panel.

I.T.S Technologies. (2023b). *Solar panel comparison – ITS Technologies*. [online] Available at: https://www.itstechnologies.shop/pages/solar-panel-comparison [Accessed 5 Dec. 2023].

IEC (2023) *Transmission distribution*. Available at: https://www.iec.ch/energies/transmission-distribution#:~:text=Power%20transmission%20is%20the%20large,%2C%20public%2C%20and%20industrial%20customers. (Accessed: 28 November 2023).

IEP (2023) *Why is voltage stepped up only to be stepped down?*, *Imperia Engineering Partners*. Available at: https://imperiaep.com/why-is-voltage-stepped-up-only-to-be-stepped-down/ (Accessed: 11 December 2023).

IRENA (2020). *30 YEARS OF POLICIES FOR WIND ENERGY*. [online] Available at: https://www.irena.org/-/media/Files/IRENA/Agency/Publication/2013/GWEC/GWEC_Portugal.pdf?la=en&hash=9AC1FCF27CBEF69846F1FDDBCE5434E2DD79267F [Accessed 1 Dec. 2023].

Kaplan, U., Nathan, A. and Ponte, C., (2007). Pico Vermelho geothermal project, Azores, Portugal. *Geothermal Resources Council Transactions*, *31*, pp.521-524. Available at: https://publications.mygeoenergynow.org/grc/1025271.pdf

LuvSide (2020). *7 Advantages of Vertical Axis Wind Turbines (VAWT) | The Windy Blog*. [online] https://www.luvside.de/en/. Available at: https://www.luvside.de/en/vawt-advantages/ [Accessed 13 Nov. 2023].

M. H. Saeed, W. Fangzong, B. A. Kalwar and S. Iqbal, "A Review on Microgrids' Challenges & Perspectives," in IEEE Access, vol. 9, pp. 166502-166517, 2021, doi: 10.1109/ACCESS.2021.3135083.

Meister, P., Jia, H., Li, J., Kloepsch, R., Winter, M. and Placke, T. (2016). Best Practice: Performance and Cost Evaluation of Lithium Ion Battery Active Materials with Special Emphasis on Energy Efficiency. *Chemistry of Materials*, 28(20), pp.7203–7217. doi:https://doi.org/10.1021/acs.chemmater.6b02895.

Melo, F. (2020) *Characterisation and evolution of the Azorean electrical system. The cases of São Miguel and the central islands of Faial, Pico and São Jorge*. rep.

Meshram, P., Mishra, A., Abhilash and Sahu, R. (2020). Environmental impact of spent lithium ion batteries and green recycling perspectives by organic acids – A review. *Chemosphere*, 242, p.125291. doi:https://doi.org/10.1016/j.chemosphere.2019.125291.

meteoblue. (2023). *Simulated historical climate & weather data for Azores*. [online] Available at: https://www.meteoblue.com/en/weather/historyclimate/climatemodelled/azores_portugal_3373385 [Accessed 8 Dec. 2023].

Mongird, K., Viswanathan, V., Balducci, P., Alam, J., Fotedar, V., Koritarov, V. and Hadjerioua, B. (2020). An Evaluation of Energy Storage Cost and Performance Characteristics. *Energies*, 13(13), p.3307. doi:https://doi.org/10.3390/en13133307.

NASA. (1979). *MODIFIED POWER LAW EQUATIONS FOR VERTICAL WIND PROFILES*. [online] Available at: https://ntrs.nasa.gov/api/citations/19800005367/downloads/19800005367.pdf.

National Grid (2023) *Distribution and transmission connections- what's the difference?*, *Distribution and transmission connections- what's the difference? | National Grid ET*. Available at: https://www.nationalgrid.com/electricity-transmission/connections/article/distribution-and-transmission-connections#:~:text=The%20transmission%20network%20is%20responsible,down%20to%20132kV%20and%20below. (Accessed: 4 December 2023).

NREL (2013). *SAM/deploy/libraries/CEC Modules.csv at develop · NREL/SAM*. [online] GitHub. Available at: https://github.com/NREL/SAM/blob/develop/deploy/libraries/CEC%20Modules.csv [Accessed 5 Dec. 2023].

Penn State. (2023). *Wind Energy and Power Calculations | EM SC 470: Applied Sustainability in Contemporary Culture*. [online] Available at: https://www.e-education.psu.edu/emsc297/node/649 [Accessed 13 Nov. 2023].

Pimentel, P., Oliveira, A., Couto, G., Ponte, J.C. and Castanho, R. (2020). *The Azores Archipelago as a Region with Vast Potential for the Development of Adventure and Slow Tourism*. [online] www.intechopen.com. Available at: https://www.intechopen.com/chapters/73861.

Pimm, A.J., Cockerill, T.T. and Taylor, P.G. (2018). The potential for peak shaving on low voltage distribution networks using electricity storage. *Journal of Energy Storage*, 16(1), pp.231–242. doi:https://doi.org/10.1016/j.est.2018.02.002.

PV Performance Modeling Collaborative (PVPMC). (n.d.). *Angle of Incidence*. [online] Available at: https://pvpmc.sandia.gov/modeling-guide/1-weather-design-inputs/plane-of-array-poa-irradiance/calculating-poa-irradiance/angle-of-incidence/.

Rangel, M.D.G. (2020) 'The Azores archipelago: powered by geothermal', *CommUnity Post Magazine | 3rd Edition*. Available at: https://issuu.com/communitybyinnoenergy/docs/3rd_mag_online/s/10320975 (Accessed: 12 November 2023).

Reda, I. and Andreas, A. (2004). Solar position algorithm for solar radiation applications. *Solar Energy*, 76(5), pp.577–589. doi:https://doi.org/10.1016/j.solener.2003.12.003.

Renewableshop.co.uk. (2023). *Solplanet 100kW, 3ph 10MPPT Inverter, WiFi-Stick, With DC*. [online] Available at: https://renewableshop.co.uk/products/solplanet-100kw-3ph-10mppt-inverter-wifi-stick-with-dc [Accessed 5 Dec. 2023].

rye.esmclients.com. (2021). *The Importance of Local Labour - RYE Demolition*. [online] Available at: https://www.ryegroup.co.uk/blog/engaging-local-labour-in-demolition/.

Sadler, R. (2023). *Solar panels UK cost and prices 2023 | The Independent*. [online] Independent Advisor. Available at: https://www.independent.co.uk/advisor/solar-panels/solar-panel-cost#:~:text=Solar%20panel%20labour%20costs&text=Solar%20panel%20labour%20costs%20are [Accessed 10 Dec. 2023].

Siemens (2023) *Siemens completes Azores Sustainable Power Project, creating a Blu ..., Press*. Available at: https://press.siemens.com/global/en/pressrelease/siemens-completes-azores-sustainable-power-project-creating-blueprint-other-islands (Accessed: 29 November 2023).

Six Senses. (2022). *Six Senses Ninh Van Bay Switches on the Sun*. [online] Available at: https://www.sixsenses.com/en/corporate/media-center/press-releases/2022/six-senses-ninh-van-bay-ninh-van-greens-solar-farm#:~:text=As%20of%20August%202022%2C%20Ninh,to%20feed%20guests%20and%20hosts [Accessed 9 Nov. 2023].

Smoot, G. (2023). *What Is the Carbon Footprint of Wind Energy? A Life-Cycle Assessment*. [online] Impactful Ninja. Available at: https://impactful.ninja/the-carbon-footprint-of-wind-energy/ [Accessed 4 Dec. 2023].

Solargis (2020). *Global Solar Atlas*. [online] Globalsolaratlas.info. Available at: https://globalsolaratlas.info/map.

Solaris Renewables. (2022). *What Is the Carbon Footprint of Solar Panel Manufacturing?* [online] Available at: https://solarisrenewables.com/blog/what-is-the-carbon-footprint-of-solar-panel-manufacturing/#:~:text=Solar%20panels%20emit%20around%2050g [Accessed 5 Dec. 2023].

Souka, A.F. and Safwat, H.H. (1966). Determination of the optimum orientations for the double-exposure, flat-plate collector and its reflectors. *Solar Energy*, 10(4), pp.170–174. doi:https://doi.org/10.1016/0038-092x(66)90004-1.

Stehly, T. and Duffy, P. (2022). *2021 Cost of Wind Energy Review*. [online] Available at: https://www.nrel.gov/docs/fy23osti/84774.pdf [Accessed 23 Nov. 2023].

Tierra Atacama. (2023). *Tierra Atacama Sustainability Efforts | Tierra Atacama Hotel*. [online] Available at: https://tierraatacama.com/sustainability/ [Accessed 9 Nov. 2023].

Tjiu, W., Marnoto, T., Mat, S., Ruslan, M.H. and Sopian, K. (2015). Darrieus vertical axis wind turbine for power generation I: Assessment of Darrieus VAWT configurations. *Renewable Energy*, 75, pp.50–67. doi:https://doi.org/10.1016/j.renene.2014.09.038.

Tye, H. (2023). *Tree-inspired wind turbine foundation could reduce CO2 emissions by 80%*. [online] Building Design. Available at: https://www.bdonline.co.uk/buildings-design-and-specification/tree-inspired-wind-turbine-foundation-could-reduce-co2-emissions-by-

80/5123757.article#:~:text=Tree%2Dinspired%20wind%20turbine%20foundation%20could%20reduce%20CO2%20emissions%20by%2080%25 [Accessed 5 Dec. 2023].

Uddin, M., Mo, H., Dong, D., Elsawah, S., Zhu, J. and Guerrero, J.M., 2023. Microgrids: A review, outstanding issues and future trends. *Energy Strategy Reviews*, *49*, p.101127.

Weterings, R., Bastein, T., Tukker, A., Rademaker, M. and Ridder, M. de (2013). *Resources for our Future: Key issues and best practices in Resource Efficiency*. [online] *Google Books*. The Hague Centre for Strategic Studies. Available at: https://books.google.co.uk/books?hl=en&lr=&id=indeBAAAQBAJ&oi=fnd&pg=PA9&dq=global+best+practices+in+waste+reduction+and+resource+efficiency&ots=nwB4eUk6H6&sig=vCXtkYQ9VOLCsN5eYUbZGKorhNA&redir_esc=y#v=onepage&q=global%20best%20practices%20in%20waste%20reduction%20and%20resource%20efficiency&f=false [Accessed 12 Dec. 2023].

WINDPOWER. (2010). *Wind Wire: Portugal - Investment for Azores islands*. [online] Available at: https://www.windpowermonthly.com/article/994684/wind-wire-portugal-investment-azores-islands [Accessed 1 Dec. 2023].

Wiser, R., Bolinger, M. and Seel, J. (2020). *Benchmarking Utility-Scale PV Operational Expenses and Project Lifetimes: Results from a Survey of U.S. Solar Industry Professionals*. [online] Available at: https://eta-publications.lbl.gov/sites/default/files/solar_life_and_opex_report.pdf.

Wood, E. (2023) *What is a microgrid?*, *Microgrid Knowledge*. Available at: https://www.microgridknowledge.com/about-microgrids/article/11429017/what-is-a-microgrid (Accessed: 11 December 2023).

World Tourism Organization (2011). Analysis on Energy Use by European Hotels – Online Survey and Desk Research. doi:https://doi.org/10.18111/9789284414970.

7 Appendices

Appendix A: Fast sketch and layout proposal for ECO-resort

1 : pool and bar (restaurant) area overlooking atlantic ocean (infinity pool 54 × 82 ft) 450 sq ft.

2- 8 : coastal villas that look out onto sea (30 × 55 ft = 1650 sq ft)

9-10 : coastal retreat villas (35 x 60) 2100 sq ft

11- 13 : mountain retreat villas (35 x 60) 2100 sq ft raised up with jacuzzi on balcony

14 - 18 : family villas with 2 bedrooms and own private pool (40 ft x 65) 2600 sq ft.

19 : 2nd, but main restaurant with lovely coastal view (80 x 100) 8000 sq ft bar also in area

20 : Spa (adding to the luxury side of the resort)

⊗ : potential site for solar panels and organic garden which provides fruit and veg for hotel

* Important details
- 100 ft space between pool area and first villa
- 15 ft between each coastal villa
- 40 ft between restaurant and villas either side
- 30 ft between each retreat villa

Appendix B: Solar Energy Output Modelling in Python Code

```python
# Importing necessary libraries
import pvlib
from pvlib.location import Location
import pandas as pd
import matplotlib.pyplot as plt
from pvlib.pvsystem import PVSystem, Array, SingleAxisTrackerMount
from energy_demand import hotel_energy_consumption
import numpy as np

# Setting font family for plots
plt.rc('font', family='Helvetica')

# Defining module parameters
celltype = "monoSi"
pdc0 = 410
v_mp = 31.2
i_mp = 13.15
v_oc = 37.2
i_sc = 14.01
alpha_sc = 0.0005 * i_sc
beta_voc = -0.0026 * v_oc
gamma_pdc = -0.37
cells_in_series = 108
temp_ref = 25

# Creating a location object for Azores
location = Location(latitude=37.8372, longitude=-25.3700, tz='Atlantic/Azores', altitude=65.53, name='Azores shoreside')
surface_tilt = 27
surface_azimuth = 180

# Setting start and end times for simulation
start ="2023-07-01 00:00"
end = "2023-07-05 00:00"

# Reading POA (Plane of Array) data from a CSV file and filtering based on the specified time range
poa_data_2020 = pd.read_csv('poa_data_2020.csv', index_col=0)
poa_data_2020.index = pd.date_range(start="2023-01-01 00:00", periods=len(poa_data_2020.index), freq='1h')
poa_data = poa_data_2020[start:end]

# Calculating solar position, angle of incidence, incidence angle modifier, effective irradiance, and cell temperature
solarpos = location.get_solarposition(times=pd.date_range(start=start, end=end, freq='1h'))
aoi = pvlib.irradiance.aoi(surface_tilt, surface_azimuth, solarpos.apparent_zenith, solarpos.azimuth)
iam = pvlib.iam.ashrae(aoi)
effective_irradiance = poa_data["poa_direct"] * iam + poa_data["poa_diffuse"]
temp_cell = pvlib.temperature.faiman(poa_data["poa_global"], poa_data["temp_air"], poa_data["windspeed"])
```

```python
# Fitting CEC (California Energy Commission) parameters for the PV module
I_L_ref, I_o_ref, R_s, R_sh_ref, a_ref, Adjust = pvlib.ivtools.sdm.fit_cec_sam(
    celltype=celltype,
    v_mp=v_mp,
    i_mp=i_mp,
    v_oc=v_oc,
    i_sc=i_sc,
    alpha_sc=alpha_sc,
    beta_voc=beta_voc,
    gamma_pmp=gamma_pdc,
    cells_in_series=cells_in_series,
    temp_ref=temp_ref
)

# Calculating CEC parameters for the effective irradiance and cell temperature
cec_params = pvlib.pvsystem.calcparams_cec(effective_irradiance, temp_cell, alpha_sc, a_ref, I_L_ref, I_o_ref, R_sh_ref, R_s, Adjust)

# Calculating maximum DC power point using the Newton-Raphson method
mpp = pvlib.pvsystem.max_power_point(*cec_params, method='newton')

# Creating a PV system object and scaling voltage, current, and power based on the calculated maximum power point
system = PVSystem(modules_per_string=20, strings_per_inverter=12)
dc_scaled = system.scale_voltage_current_power(mpp)

# Retrieving inverter information from the SAM (System Advisor Model) database
inverters = pvlib.pvsystem.retrieve_sam('CECInverter')
inverter = inverters['ABB__ULTRA_1100_TL_OUTD_3_US_690_x_y_z__690V_']

# Calculating AC energy output using the Sandia inverter model
ac_results = pvlib.inverter.sandia(
    v_dc=dc_scaled.v_mp,
    p_dc=dc_scaled.p_mp,
    inverter=inverter
)
```

Appendix C: Solar Module Parameters

Cell Type	Monocrystalline Silicon
Area	1.953
P_{dc0}	410W
Operating Voltage	31.2V
Operating Current	13.15A
Open Circuit Voltage	37.2V
Short Circuit Current	14.01V
Temperature Coefficient (Short Circuit Current)	0.0005 C^{-1}
Temperature Coefficient (Open Circuit Voltage)	0.007 C^{-1}
Temperature Coefficient (Maximum Power) (γ_{pdc})	-0.37 C^{-1}
Cells in series	108

Appendix D: Validation of Floris

Appendix D: Validation 1

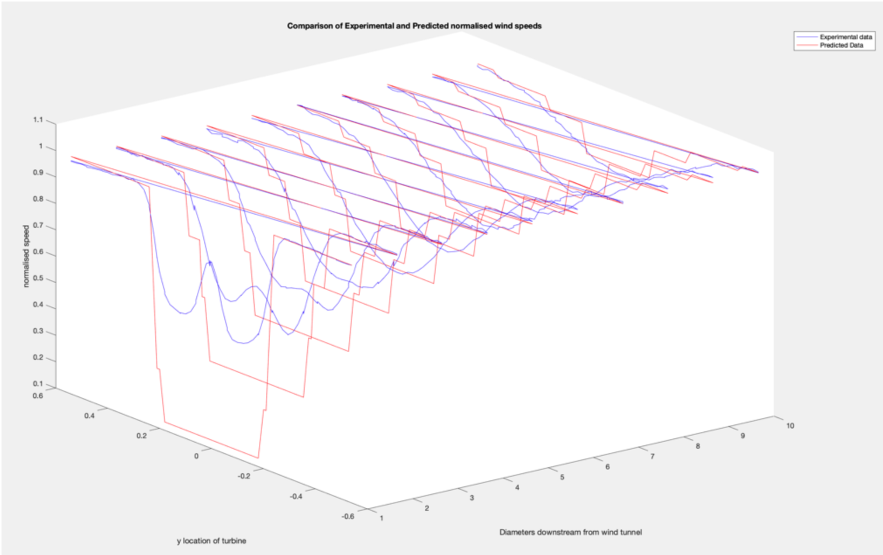

Appendix D: Validation 2

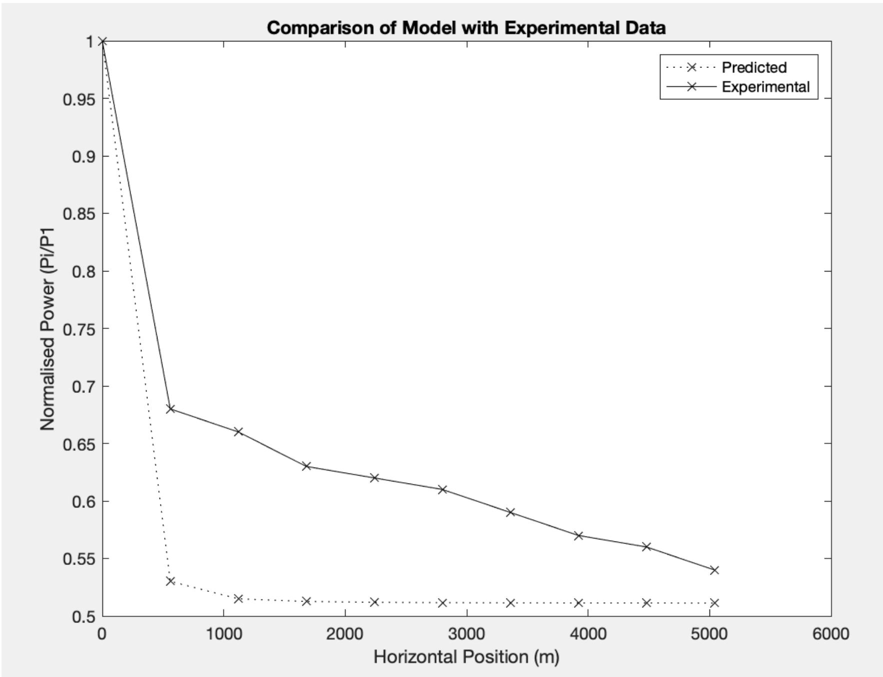

Appendix E: Equations for Wind

$$V_w(h) = V_{10} \times \left(\frac{h}{h_{10}}\right)^{\alpha}$$

vw(h)= velocity of the wind [m/s], at height, h [m],v10= velocity of the wind [m/s], at height,h10 = 10m ,α= Hellmann exponent

$$\mathrm{P} = 1/2\rho v^3 A$$

ρ is the air density(kg/m3), v is wind velocity (m/s), A is effective area of the rotors/disk (m2).

$$\mu = (1 - k_m) * (1 - ke) * (1 - ke,t) * (1 - kt) * (1 - kw) * C_p.$$

C_p is the turbine efficiency. It must be lower than the Betz limit (59.3%), and is typically between 30- 40% , kw are the wake losses due to neighbouring turbines and the terrain topography, typically 3-10% , k_m are the mechanical losses of the blades and gearbox, typically 0-0.3% , ke are the electrical losses of the turbine, typically 1-1.5% , ke,t are the electrical losses of transmission to grid, typically 3-10% , kt is the percentage of time out of order due to failure or maintenance, typically 2-3% , μ is the efficiency.